FUNCTIONAL LAYERED MATERIALS FOR CHEMICAL DETECTION USING SURFACE-ENHANCED RAMAN SPECTROSCOPY

BY

THITIMA MATUROS DANIELS

A DISSERTATION SUBMITTED IN PARTIAL FULFILLMENT OF THE REQUIREMENTS FOR THE DEGREE OF DOCTOR OF PHILOSOPHY (ENGINEERING AND TECHNOLOGY)

SIRINDHORN INTERNATIONAL INSTITUTE OF TECHNOLOGY

THAMMASAT UNIVERSITY

ACADEMIC YEAR 2022

Ref. code: 25655922300099OUH

THAMMASAT UNIVERSITY

SIRINDHORN INTERNATIONAL INSTITUTE OF TECHNOLOGY

DISSERTATION

BY

THITIMA MATUROS DANIELS

ENTITLED

FUNCTIONAL LAYERED MATERIALS FOR CHEMICAL DETECTION USING SURFACE-ENHANCED RAMAN SPECTROSCOPY

was approved as partial fulfillment of the requirements for
the degree of Doctor of Philosophy (Engineering and Technology)

on January 4, 2022

Chairperson _____
(Anurat Wisitsora-at, Ph.D.)

Member and Advisor _____
(Associate Professor Paiboon Sreearunothai, Ph.D.)

Member and Co-advisor _____
(Noppadon Nuntawong, Ph.D.)

Member _____
(Assistant Professor Shu-Han Hsu, Ph.D.)

Member _____
(Associate Professor Pakorn Opaprakasit, Ph.D.)

Director _____
(Professor Pruettha Nanakorn, D.Eng.)

Dissertation Title	FUNCTIONAL LAYERED MATERIALS FOR CHEMICAL DETECTION USING SURFACE-ENHANCED RAMAN SPECTROSCOPY
Author	Thitima Maturos Daniels
Degree	Doctor of Philosophy (Engineering and Technology)
Faculty/University	Sirindhorn International Institute of Technology/ Thammasat University
Dissertation Advisor	Associate Professor Paiboon Sreearunothai, Ph.D.
Dissertation Co-Advisor	Noppadon Nuntawong, Ph.D.
Academic Years	2022

ABSTRACT

Surface-enhanced Raman scattering (SERS) is one of the useful techniques for identifying a specific fingerprint of molecules. Conventional SERS consists of colloid based and thin film-based types. The colloid-based SERS uses a nanoparticle metal colloid to enhance the Raman signal of the target molecules while the thin film SERS uses coating technique to make a cluster of metal nanoparticles on the substrate to enhance the Raman signal. The challenge in developing the thin film-based SERS technique besides the sensitivity is the improvement of the reproducibility and stability of the SERS substrate. In this work, a graphene/Ag-nanoparticle/polymer (G/AgNP/polymer) SERS substrate was successfully fabricated using chemical vapor deposition (CVD), electrodeposition, transferring, and etching techniques. CVD was used for growing a graphene layer on a copper foil substrate. Graphene functions as a protective layer of the SERS substrate and help enhance Raman signal via chemical enhancement. Silver nanoparticles as an enhancement material were coated on graphene by electrodeposition technique. The structure of the silver nanoparticles growth on the graphene/copper substrate can be tuned by varying the electrodeposition condition to obtain proper ‘hot spot’ for Raman amplification. The electrodeposition condition at

Ref. code: 25655922300099OUH

the current density of 10 uA cm^{-2} for 3 min generates a rattan ball-like structure of the Ag nanoparticles with the gaps between metal nanoparticles between 30-100 nm. The as-prepared layers were then transferred onto two types of polymer substrates which are polyimide (PI) tape and polydimethylsiloxane (PDMS) substate. The copper layer was etched out using a ferric chloride solution ($FeCl_3$). The developed SERS substrate could detect methyl parathion with the enhancement factor (EF) of the primary peak at 1344 cm^{-1} of $1.5x10^4$ and $4.7x10^4$ for the PMDS and PI SERS substrates, respectively. Compare between two types of substrates, PDMS SERS substrate shows better enhancement factor, while the uniformity of the prepared PI SERS substrate was better than that of the PDMS SERS substrate. The shelf life of both SERS substrates were longer than 48 days at room temperature, thanks to the protective graphene layer, making the developed SERS substrate practical for field use. The developed technique offers a facile fabrication with low cost and ease of SERS storage without additional packaging process. This polymer-based SERS substrate is a promising platform with potential for use as a screening technique in field tests.

Keywords: SERS, Flexible substrate, Graphene, Silver nanostructure, Polyimide tape, Electrodeposition, Methyl parathion

Ref. code: 25655922300099OUH

ACKNOWLEDGEMENTS

The success of this thesis has been attributed to the extensive support and great encouragement from my major advisor, Assist. Prof. Dr. Paiboon Sreearunothai. My gratitude also thanks to Dr. Noppadon Nuntawong my co-advisor, for his kindness assistance in examining the research instrument and suggestion. I deeply thank them for their valuable advice and guidance in this thesis.

I am grateful to express my sincere thanks to Assist. Prof. Dr. Pakorn Opaprakasit, Dr. Anurat Wisitsorraat, Dr. Shu-Han Hsu for providing their comments and discussions.

I greatly appreciate all my friends and staff of the Department of Common and Graduate Studies in particular, Ms. Gladis Aros. Safitri, Mr. Thilina Rajeendre, Mrs. Naree Chankeaw and all other, for their kind support and cheerfulness.

Thank you to the members of OEC research team for providing helpful comments and suggestions.

Finally, I would like to express my sincere gratitude to my family for their patience and encouragement.

Thitima Maturos Daniels

Ref. code: 25655922300099OUH

TABLE OF CONTENTS

	Page
ABSTRACT	(1)
ACKNOWLEDGEMENTS	(3)
LIST OF TABLES	(7)
LIST OF FIGURES	(8)
LIST OF SYMBOLS/ABBREVIATIONS	(11)
CHAPTER 1 INTRODUCTION	
1.1 Background	1
1.2 Statement of the problems	2
1.3 Objectives of the research	2
1.4 Outline of the thesis	2
CHAPTER 2 REVIEW OF LITERATURE	3
2.1 Raman spectroscopy	3
2.2 Surface-Enhanced Raman Spectroscopy (SERS)	4
2.2.1 SERS enhancement mechanisms	6
2.2.1.1 Chemical enhancement	6
2.2.1.2 Electromagnetic enhancement	7
2.3 Film-based SERS fabrication	8
2.3.1 Etching/patterning method	8
2.3.2 Physical deposition	9
2.3.2.1 Sputtering	9
2.3.2.2 Pulse laser deposition	10
2.3.2.3 Evaporation	11

Ref. code: 25655922300099OUH

2.3.3 Chemical deposition 12
2.3.3.1 Chemical vapor deposition 13
2.3.3.2 Electrophoretic deposition 14
2.4 Graphene for SERS application 15
2.5 Flexible SERS 17
2.6 Summary 18

CHAPTER 3 METHODOLOGY 19
3.1 Preparation of flexible SERS substrate 19
3.1.1 Preparation of graphene on a copper foil substrate 20
3.1.2 Electrodeposition of silver nanoparticles on graphene 21
3.1.3 Preparation of polymer protective layer onto the Ag-decorated graphene 22
3.1.3.1 PDMS coating 22
3.1.3.2 Polyimide tape 23
3.2 Characterizations 24
3.3 Study of the SERS performance 25
3.4 Data pre-processing and analysis of Raman spectrum 26

CHAPTER 4 RESULTS AND DISCUSSION 28
4.1 Characterizations of graphene/copper foil substrate 28
4.2 Effect of current density and deposition time to silver nanoparticle morphology 35
4.3 Effect of excitation light source to Raman measurement 39
4.4 Effect of current density and deposition time to SERS performance 43
4.5 Effect of graphene and the enhancement mechanisms 45
4.6 Sensitivity of SERS substrate 46
4.7 Uniformity of SERS substrate 47
4.8 Stability of SERS substrate 51
4.9 Testing SERS substrate with real sample 54
4.10 Suggestions for Future Research 58

Ref. code: 25655922300099OUH

4.10.1 Additional polymer-based SERS 58
4.10.2 Preparation of Ag nanoparticle by sputtering technique 60
4.10.3 AgO elimination 61
4.11 Summary 61

CHAPTER 5 CONCLUSIONS 63

REFERENCES 66

APPENDICES
APPENDIX A 72
APPENDIX B 74

BIOGRAPHY 75

Ref. code: 25655922300099OUH

LIST OF TABLES

Tables	Page
4.1 Comparison of atomic concentration of silver phase of each SERS substrate	33
4.2 Comparison of the mechanical properties of bare PI and PI SERS substrate	39
4.3 Recovery test of methyl parathion on apple	58

Ref. code: 25655922300099OUH

LIST OF FIGURES

Figures	Page
2.1 The schematic diagram of photon scattering with elastic and inelastic scattering	3
2.2 Scheme of Raman spectroscopy	4
2.3 Energy diagram showing the possible charge transfer in case of metal surface and analyte molecule and dielectric surface and analyte molecule	7
2.4 DC magnetron sputtering system	10
2.5 Pulse laser deposition system	11
2.6 Evaporation system	12
2.7 Chemical Vapor Deposition (CVD) system	13
2.8 Electrophoretic deposition setup	15
3.1 Schematic illustration of the process for the fabrication of the G/AgNPs/Polymer substrate and the potential use of the developed substrate	19
3.2 Mechanism of growing graphene on the copper substrate and the CVD system used for growing graphene in this work	20
3.3 Electrodeposition of silver nanoparticles onto graphene/Cu substrate. The image on the left is the graphene/Cu before electrodeposition. Image on the right is after electrodeposition showing the deposited the silver layer deposited on the surface of the graphene/Cu substrate	21
3.4 The PDMS precursor together with its curing agent and the polyimide tape used in this work	22
3.5 Picture of G/Ag/PDMS SERS substrate and G/Ag/PI SERS substrate	24
3.6 Molecular structure of methyl parathion	26
4.1 Raman spectra of graphene on copper foil	28
4.2 XRD pattern of silver prepared by electrodeposition technique	29
4.3 The wide scan of XPS spectra and the detailed scan of Ag 3d and O 1s component of Ag/G/Cu, PDMS/Ag/G, Ag/PDMS, G/Ag/PI and Ag/PI	32

Ref. code: 25655922300099OUH

4.4 The intensity mapping plot of the G band (1582 cm^{-1}) of graphene performed on PDMS and PI SERS substrate 34
4.5 FE-SEM images of silver nano particle prepared by the electrodeposition method at current densities of 1, 5, 10, 20, 50, 100 $\mu A/cm^2$ for 180 s on a graphene/Cu substrate 37
4.6 FE-SEM images of AgNPs preparing by electrodeposition method at current density of 10 $\mu A/cm^2$ for 30 s, 120 s, 180 s, and 300 s 38
4.7 The stress–strain plot of G/AgNPs/PI substrate compared to that of pristine PI SERS substrate. 39
4.8 Absorbance of PDMS and PI substrate 40
4.9 Raman spectra of methyl parathion on G/Ag/PDMS obtaining from 785 nm and 532 nm excitation laser source 41
4.10 Raman spectra of PDMS substrate, methyl parathion on PDMS substrate, methyl parathion on G/Ag/PDMS SERS substrate and methyl parathion powder obtained by the 532 nm excitation source 42
4.11 Raman spectra of the PI substrate, methyl parathion on PI substrate, methyl parathion on G/Ag/PI SERS substrate and methyl parathion powder obtained by the 785 nm excitation source 43
4.12 Intensity of Raman signal from SERS substrate at different electrodeposition current densities and deposition times 44
4.13 The intensity of the Raman signal at wave number 1344 cm^{-1} obtained by PDMS and PI SERS substrate with and without graphene coverage 45
4.14 Linear relationship between methyl parathion concentration and the normalized intensity of the Raman signal at wave number 1344 cm^{-1} 47
4.15 Plot of Raman spectra and Raman intensity at 1,344 cm^{-1} of each spot for the PMDS SERS substrate. At 1,344 cm^{-1}, the %RSD relative to the mean intensity was calculated to be 25%. 49
4.16 Plot of Raman spectra and Raman intensity at 1,344 cm^{-1} of each spot for the PI SERS substrate. At 1,344 cm^{-1}, the %RSD relative to the mean intensity was calculated to be 11%. 50

Ref. code: 25655922300099OUH

4.17 The Raman intensity at wave number 1344 cm^{-1} of the PDMS SERS substrate as a function of storage time under the ambient air and under a desiccator at 25 °C and 40%RH 52
4.18 The Raman intensity at wave number 1344 cm^{-1} of the PI SERS substrate as a function of storage time under the ambient air and under a desiccator at 25 °C and 40%RH 53
4.19 Raman spectra of methyl parathion residue on apple detected by PDMS SERS substrate 55
4.20 Raman spectra of methyl parathion residue on apple detected by PI SERS substrate 56
4.21 Linear relationship between methyl parathion concentration and the normalized intensity of the Raman signal at wave number 1344 cm^{-1} of Raman signal on apple 57
4.22 Raman signal of 1 mM Methyl parathion measuring by SERS substrate preparing with clear tape, net tape, and very high bond tape (VHB tape) 59
4.23 FE-SEM images of silver nanoparticle preparing by sputtering method at an applied current of 0.2 A for 5 s, 15 s, 30 s, and 60 s and Raman signal of methyl parathion on the SERS substrate preparing by various sputtering time 60
4.24 FE-SEM images of silver nanoparticle on graphene/Cu substrate and after hydrogen treatment 61

Ref. code: 25655922300099OUH

LIST OF SYMBOLS/ABBREVIATIONS

Symbols/Abbreviations	Terms
Ag	Silver
$AgNO_3$	Silver nitrate
Au	Gold
Ar	Argon
Cu	Copper
DI	Distilled Water
EF	Enhancement factor
EM	Electromagnetic
FE-SEM	Field emission scanning electron microscope
HOMO	Highest occupied molecular orbital
LSPR	Localized surface plasmon resonance
LUMO	Lowest unoccupied molecular orbital
NIR	Near-infrared radiation
PDMS	Polydimethylsiloxane
PI	Polyimide
PVD	Physical vapor deposition
SERS	Surface-Enhanced Raman Scattering
SEM	Scanning Electron Microscope
SiO_2	Silicon dioxide
TiO_2	Titanium dioxide
XRD	X-ray diffraction

Ref. code: 25655922300099OUH

CHAPTER 1
INTRODUCTION

1.1 Background

Raman spectroscopy or Raman scattering is a technique that observes the scattering of the light interacting with the molecules due to the vibration of those molecules. This scattering is unique and can be used as a tool to define a fingerprint of each molecule. However, the limitation of this technique for an identified material is that the Raman signal is typically weak and thus difficult to collect the signal. Surface-enhanced Raman spectroscopy or surface-enhanced Raman scattering is a surface sensitive technique that enhances the Raman signal by using adsorption of molecules on a rough metal surface. The metal used for Raman enhancement is Ag, Au, Cu. SERS can be divided into two groups; colloidal based and film based. Although colloidal-based SERS is a sensitive technique with high specificity, the limitations found in this technique are the aggregation of the colloid, complication of preparing the colloid and storing samples make it inconvenient for field tests. Film-based SERS are now widely used to overcome those problems. The film-based SERS uses a rough metal surface pattern on the substrate to avoid an aggregate problem. The various substrates for film-based SERS have been reported for example glass slide, paper, silicon wafer, filter paper, etc.(Li et al., 2010; Li et al., 2013). However, the problem with film-based SERS is oxidation on the metal surface, thus special films, or treatments with chemically inert materials to cover the metal surface are needed. To protect the metal surface of SERS, there are several materials have been used as a protection layer such as TiO_2 (Ma et al., 2015), SiO_2 (Zhao et al., 2016), and polymers (Wang et al., 2021). Those methods are difficult to fabricate, and some coverings will drop the Raman signal as well. Graphene is a 2D material with unique electrical and mechanical properties, high specific surface area, chemical inertness, and transparency. Graphene has been reported to be used for enhancing Raman signal via a chemical enhancement mechanism though the promotion of charge transfer ability (Ling et al., 2012). The composite of graphene and silver nanoparticle aim to improve the enhancement of Raman signal and durability of SERS substrate which can be stored at room temperature without additional packaging.

Ref. code: 25655922300099OUH

1.2 Statement of the problems

As mentioned above, the durability of film-based SERS substrates is a major concern. We would like to prepare a durable SERS substrate that provides a high enhancement ability that can be kept in normal atmosphere without additional packaging processes. The SERS substrate in this work consists of metal nanoparticles sandwiched between polymer and graphene. The polymer functions as a supporting material and graphene as a protective layer to protect against degradation on the metal surface.

1.3 Objectives of the research

The objective of the thesis is to study the preparation and characterization of the layered materials of graphene/Ag/polymer as a surface-enhanced Raman substrate (SERS) for pesticide detection. The SERS substrate was prepared by chemical vapor deposition, electrodeposition and transferring method. Two types of polymers were used in this work: polydimethylsiloxane (PDMS) and polyimide tape (PI). The optimal preparation conditions for silver nanoparticles to achieve a good Raman enhancement was investigated. The sensitivity and enhancement factor of our SERS substrate for methyl parathion detection was examined. Then the other SERS properties including stability and uniformity of SERS substrate were systematically explored and optimized. Additionally, SERS the substrate was tested with the methyl parathion residue on an apple.

1.4 Outline of the thesis

There are five chapters in this thesis. In chapter 2, the principle and literature review of Raman spectroscopy and SERS are explained. The synthesis method, device preparation and characterization method and instruments are presented in chapter 3. The properties of the SERS substrate and the study of SERS performance including sensitivity, uniformity and stability are shown in chapter 4. Finally, chapter 5 presents the conclusion of this thesis.

Ref. code: 25655922300099OUH

CHAPTER 2
REVIEW OF LITERATURE

2.1 Raman spectroscopy

Raman spectroscopy is a non-destructive technique used to determine the vibrational mode of molecules. The Raman signal obtained when an incident light from a high intensity laser reacts with molecule then light scattered is detected. There are two type of scattered light, elastic scatter at the same wavelength as the laser source which is called Rayleigh Scattering, and a small amount of light approximately 1 photon in 10 million will scatter at a different frequency with an incident photon (inelastic scattering), called Raman Scattering. If light scatters at a lower frequency than a light source, it will be called stoke Raman scattering while scattering at higher energy and frequency than that of light source is anti-stoke scattering. The schematic of each scattering type is shown in Figure 2.1. The scattering energy and frequency depend on each molecular bond vibration, for example individual bonds like C-C, C-H, C=C, group bond, and polymer vibration. Thus, Raman spectroscopy can determine the fingerprint of a molecule and it can be applied in many applications which includes biosensors, forensic science, and pharmaceutics, and agriculture etc.

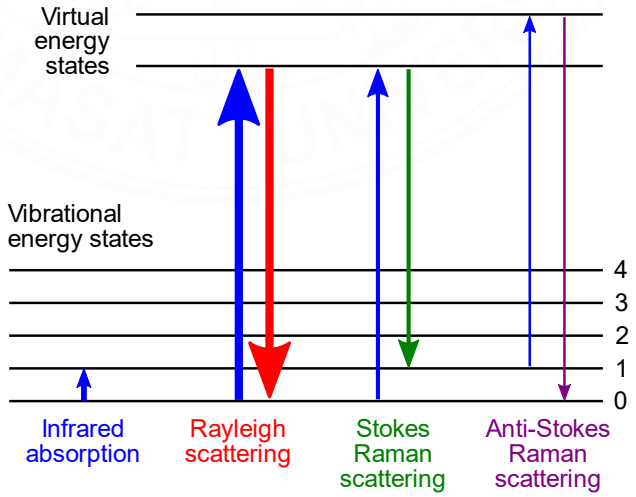

Figure 2.1 The schematic diagram of photon scattering with elastic and inelastic scattering.
(https://commons.wikimedia.org/w/index.php?curid=7845122)

Ref. code: 25655922300099OUH

A Raman spectroscopy instrument system consists of several basic components as shown in Figure 2.2. It comprises of a laser that serves as the excitation source to induce the Raman scattering. Typically, solid state lasers are used in modern Raman instruments with popular wavelengths of 532 nm, 785 nm, 830 nm and 1064 nm. The laser energy is transmitted to and collected from the sample by fiber optic cables through lens and sent to the monochromator. When the irradiation passes through the filter, the scattered light will be purified to collect only the Raman scattering and block Rayleigh scattering. A diffraction grating bends the Raman shifted light according to wavelength, and the signal is collected by CCD a detector.

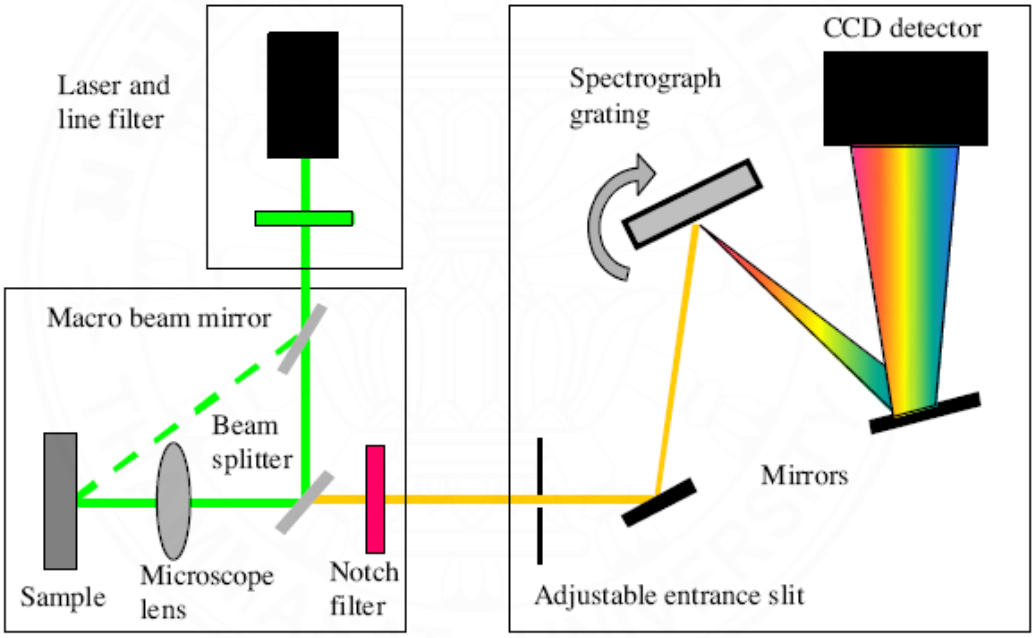

Figure 2.2 Scheme of Raman spectroscopy
(https://www.sas.upenn.edu/~crulli/TheRamanSpectrophotometer.html)

2.2 Surface-enhanced Raman spectroscopy (SERS)

According to the low Raman scattering signal from many types of molecules, the molecular analysis by this technique is limited. Surface-enhanced Raman spectroscopy or Surface-enhanced Raman scattering (SERS) was first reported by M. Fleischmann et al. in 19741 (Fleischmann et al., 1974). They observed the unusual Raman spectra of pyridine on roughened silver substrate. However, the real explanation of that phenomena as surface enhanced Raman spectroscopy (SERS) was reported by

Ref. code: 25655922300099OUH

two research groups; David L. Jeanmaire et al. (Jeanmaire & Van Duyne, 1977), and M. Grant Albrecht and J. Alan Creighton in 1977 (Albrecht & Creighton, 1977). Since then, research interest in SERS has grown exponentially. SERS is a surface-sensitive technique that enhances Raman scattering by adsorbing molecules on rough metal surfaces. The most common metals used for SERS enhancement include silver, gold, and copper. The amplification of Raman signal due to the capability of metal surface to concentrate electromagnetic energy via optical modes called surface plasmons (SPs) to enhance both the excitation and the vibration signals of molecules. The regions with intense local field enhancement are called "hot spots", which is the area that highly amplifies the usually weak Raman scattering signals. The enhancement factor for SERS can be as much as 10^{10} to 10^{15} which means that this technique may be used for single molecule detection. There are two mechanisms for explaining the enhancement behavior for SERS; electromagnetic and chemical enhancement mechanisms, which will be described later. SERS can be colloidal based where the metal nanoparticles float in three-dimensions in liquid or a film based where the metal nanoparticles align in a two-dimensional plane on a solid substrate. The enhancement in colloidal SERS is the average effect of millions of hot spots in the three-dimensional detection volume, so it usually shows a better reproducibility than that on the solid substrate which is the measurement on a small two-dimensional surface. Nevertheless, aggregation of metal colloid, limitation of hot spot and a complex preparation technique is limit usage for field testing. The film-based SERS is the patterned metal nanostructure on the surface of silicon, glass slide or another surface. The strength of the enhancement is affected by shape and size of the metal nanoparticles. The enhancement factor increases as the gap size decreases as long as the gap size is larger than the limit for the quantum effects. The enhancement efficiency of the Raman signal is defined by an enhancement factor (EF)

$$EF = \frac{I_{SERS}/N_{SERS}}{I_{NRS}/N_{NRS}} \tag{2.1}$$

Ref. code: 25655922300099OUH

Where I_{SERS} and N_{NRS} are the scattering intensities of SERS and normal Raman scattering, respectively. N_{SERS} and N_{NRS} are the number of SERS and normal Raman probe, respectively.

2.2.1 SERS enhancement mechanism

2.2.1.1 Chemical enhancement

The chemical enhancement is due to the improvement of charge transfer between substate and analyze molecules. The enhancement factor of the chemical mechanism is around 10^1-10^3. The chemical enhancement mechanism can describe only chemisorption, the physisorption or physical adsorption is not involved in the process. The several kinds of charge transfers can be the charge transfer transition between highest occupied molecular orbital (HOMO) of analyte molecules and the fermi level of metal in case of a metal substrate as shown in Figure 2.3 (a). For dielectric substrates, charge transfer transitions can be between the HOMO of molecules and the conduction band (CB) edge of substrate material or valence band (VB) of substrate material and lowest unoccupied molecular orbital (LUMO) of molecules. Moreover, electronic transition from HOMO to LUMO or transition between VB and CB of substrate material can also contribute to the enhancement of Raman signal by resonance processes. The energy diagram of the charge transfer transition shown in Figure 2.3(b) is an example of charge transfer between R6G and tungsten oxide (WS2) substrate.

Ref. code: 25655922300099OUH

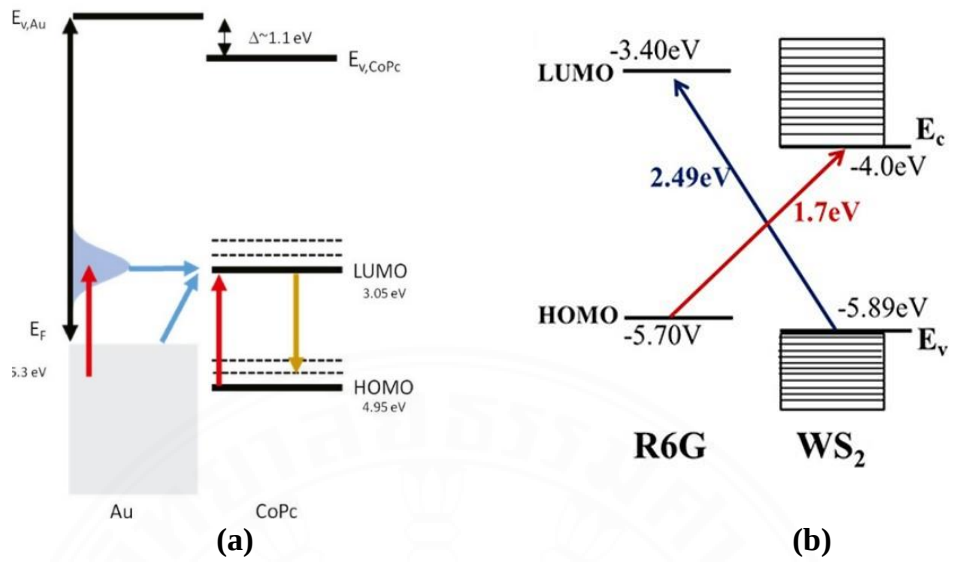

Figure 2.3 Energy diagram showing the possible charge transfer in case of metal surface and analyte molecule (a) (Chen et al., 2019) and dielectric surface and analyte molecule (b) (Kim et al., 2019)

2.2.1.2 Electromagnetic enhancement

Electromagnetic enhancement (EM) is the contribution of a localized surface plasmon resonance (LSPR) of the surface's substrate caused by the radiation light. EM does not need specific bonds between adsorbates and substrates like the case of chemical enhancement. It happens when the energy of laser source is in resonance with the surface plasmon energy on the surface, then the Raman response will be strongly enhanced. When surface plasmon occur, only the plasmons oscillate perpendicular to the surface contribute to the scattering. Thus, the roughened surfaces or arrangements of nanoparticles are typically designed for the SERS substrate to obtain the localized collective oscillations. The nanoparticle LSPR is generally a function of the particle size, shape, and surrounding medium. If there are other nanoparticles nearby, inter-particle coupling effects tremendously influence the LSPR position "hot spots". Raman scattering occurs with the excitation in the visible and near-infrared radiation (NIR), thus the metal material for SERS substrate needs to have plasmon resonance frequency in those wavelength ranges to maximize Raman enhancement. Silver and gold are

Ref. code: 25655922300099OUH

typical metals for SERS experiments because their plasmon resonance frequencies fall within these wavelength ranges. Other material like copper, platinum, and palladium also has an absorption spectrum falls within the acceptable range for SERS experiments. The enhancement factor from the electromagnetic enhancement can be up to 10^{13}.

2.3 Film-based SERS fabrication

Fabrication of metallic nanostructure film-based SERS has attracted much attention from researchers recently because it is more stable and repeatable than the colloidal SERS. The localized surface plasmon resonance (LSPR) on the surface generates a hot spot where its high electromagnetism promotes Raman signal amplification. The fabrication method for film-based SERS substrates must promote SERS performance, good reproducibility, cost effectiveness, and scalability. Available method to fabricate novel metallic nanostructure films include the deposition of nanostructure by physical or chemical process, and create a rough metal surface by milling or etching etc.

2.3.1 Etching/patterning method

Because the idea for a good SERS substrate is to generate the hot spot at its intense electromagnetic field, etching the metal substrate by chemical or physical means to generate a rough metal surface was used for preparing the SERS substrate. There are two ways to do so including etching the metal surface to make a rough surface or making a rough surface before coating it with metal. For example, Chaoxiong Ma et al. (Kim et al., 2019) used oxygen plasma to etch Ag film to make a rough surface AgNF as a SERS substrate. This SERS performance testing with 4MBA gives an enhancement factor of $6x10^6$ which is 30-fold better than the Ag substrate. Another report from Fangjia Chu group (Chu et al., 2018) reported another way of making a rough surface on teflon by laser ablation then dropping an Ag colloid on the substrate to generate a SERS substrate. Another similar example is the report from Changwon Lee research group (C. Lee et al., 2015) that fabricated a rough surface on PDMS using latex beads, after that they removed the beads and sputtered Ag on the rough PDMS surface.

Ref. code: 25655922300099OUH

2.3.2 Physical deposition

The physical method for film coating is based on the formation of the vaporized material to be deposited on the substrate surface. Usually, the process must be performed in a vacuum or controlled atmosphere to avoid interaction between the vapor and air. It is a process that the material goes from a condensed phase to a vapor phase and then back to a thin film condensed phase. Physical deposition consists of sputter deposition, pulse laser deposition, electron-beam deposition, evaporative deposition, cathodic arc deposition, etc. The advantage of physical deposition is a film with a high hardness, durability, and good corrosion-resistance. It is also environmentally friendly and can be used to deposit the composite or alloy film. However, the disadvantage of this technique is the requirement of a high vacuum system, water cooling system and sometimes high operating temperature. Many physical deposition techniques were reported as a preparation of a SERS substrate with Au, Ag and alloy materials. Examples of physical deposition for SERS substrates are shown below.

2.3.2.1 Sputtering

Sputtering is a common technique for preparing nano structures for SERS applications because it can control the size and shape of the nanostructure. It is a technique that uses a bombardment of high energy particles on the target and lets the target atoms deposit on a substrate. The sputtering process is shown in Figure 2.4. First, an inert gas is introduced into a vacuum chamber, then a constant DC voltage is applied between target material and substrate which will ionize Ar gas and generate plasma. The ionized Ar ions are then accelerated to bombard the target molecules at the cathode. Target atoms are ejected and travel to the anode substrate and start to condense into a film. The normal sputtering system sometimes has a strong magnet at the cathode to generate a magnetic field near the cathode to allow electron-only travel along the magnetic flux near the cathode instead of moving toward an anode substrate. This phenomenon helps prevent electrons from damaging a deposited film and confines Ar plasma only near the target. For SERS application, Jie Li et al. reported his work of fabricating a high efficiency silver decorated silver SERS substrate by sputtering technique that could enhance the Raman signal of adenine better than a silver substrate (Li & Fang, 2007). Changwon Lee et al. studied the effect of Ag sputtered film

Ref. code: 25655922300099OUH

thickness on SERS activity and found that besides roughness, the thickness of the metallic layer plays a significant role in the SERS activity (C. Lee et al., 2015).

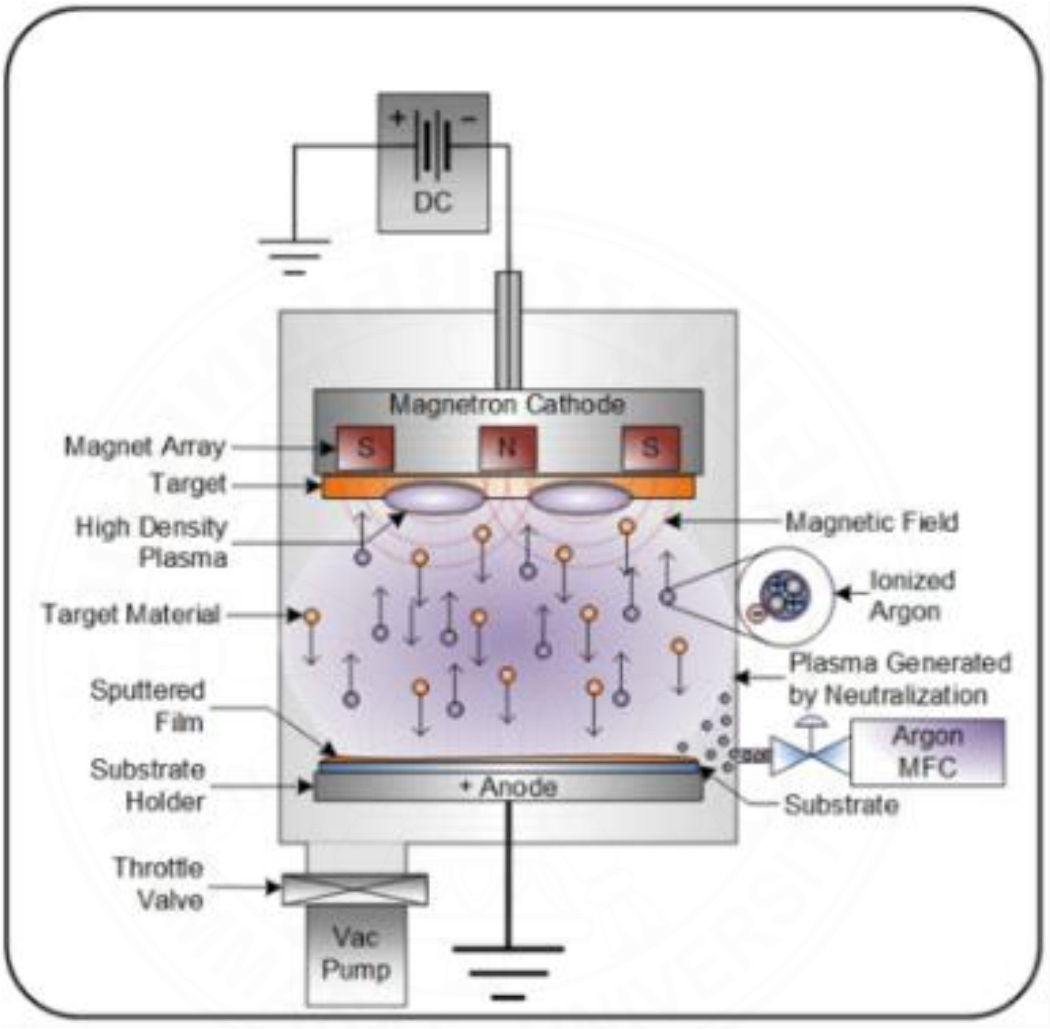

Figure 2.4 DC magnetron sputtering system

(Figure from http://www.semicore.com/what-is-sputtering)

2.3.2.2 Pulse laser deposition

Pulse laser deposition is a type of physical vapor deposition that uses a high-power laser as a source to vaporize the target material. When the laser pulse strikes the target, energy will cause an evaporation, ablation, and plasma formation. The energized species are expanded into the surrounding vacuum in the form of a plasma plume

Ref. code: 25655922300099OUH

containing many energetic species including atoms, molecules, electrons, ions, and particulates before depositing on the typically hot substrate as shown in Figure 2.5. The film formation could be controlled by varying laser wavelength, laser power, substrate temperature, pulse length, and target-sample distance. One example of preparing a SERS substrate by this technique was reported by Budner team (Budner et al., 2019) that used a pulse laser deposition method for preparing silver nano island films on Si substrate as a SERS substrate for detecting para-mercaptoaniline (pMA) molecules with an enhancement factor of 10^5.

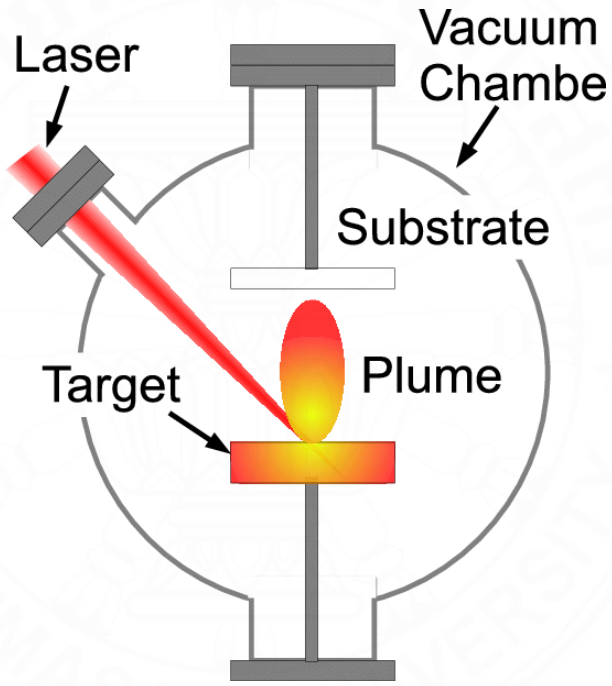

Figure 2.5 Pulse laser deposition system (Cozzens & Fox, 1978)

2.3.2.3 Evaporation

Evaporation is another technique that has been reported for preparing SERS substrates. It is a deposition technique where a source material is heated and then allowed to evaporate and condense on the substrate. An evaporation system includes a vacuum pump, crucible for the target material, heat source and substrate holder as shown in Figure 2.6. The energy source for heating the target material can be an electric

Ref. code: 25655922300099OUH

filament, electron beam, hot ceramic, or metallic bar etc. Perumal research group (Perumal et al., 2014) reported the preparation of Ag SERS substrates by E-beam evaporation that has the ability to enhance the Raman signal of 2-naphthalenethiol (NT) with the enhancement factor of 10^7. Qiang Zou et al. (Zou et al., 2018) also report E-beam evaporation of Au on a PET substrate to construct a flexible SERS substrate.

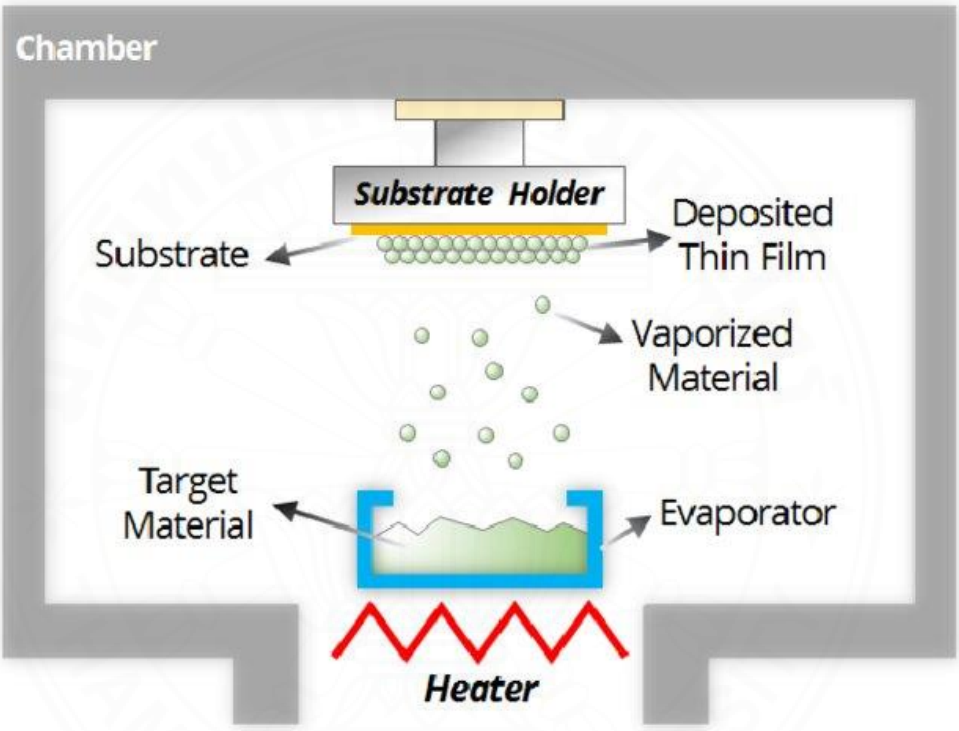

Figure 2.6 Evaporation system (Park et al., 2016)

2.3.3 Chemical deposition

Chemical deposition is the fabrication method where the material undergoes a chemical reaction resulting in a specific reaction to take place and coating on a suitable substrate. This technique can produce high-quality thin films with lower economical cost than that of physical deposition. Chemical deposition is strongly dependent on the chemistry of the solutions, pH value, viscosity, and so on. There are many chemical deposition methods that have been reported for SERS substrate fabrication including electroplating (Martynova et al., 2018), Electroless deposition (Coluccio et al., 2009;

Ref. code: 25655922300099OUH

Song et al., 2014; Tzeng et al., 2020), sol-gel technique (Lucht et al., 2000; Soto-Nieto et al., 2020), Electrophoretic deposition (Fioravanti et al., 2020; Hwang & Yang, 2018; López et al., 2013; Sarkar et al., 2014), and chemical vapor deposition (CVD) (Nakabayashi et al., 2019; Tzeng et al., 2020) etc. This section will focus on the chemical vapor deposition (CVD) and Electrophoretic deposition because they are frequently used for nanostructure fabrication.

2.3.3.1 Chemical vapor deposition

Chemical Vapor Deposition (CVD) is a deposition technique that uses heat to activate a chemical reaction of a precursor gas and allows the product to be coated on the substrate. Figure 2.7 is a schematic showing the CVD process. First, one or more precursor gases are introduced into a vacuum chamber. Applying heat or reducing pressure to vaporize those gases allows the chemical reaction to occur and deposit on a substrate. Although this technique generates a vapor to deposit on a substrate like the PVD process, CVD differs from PVD in that it is done under a chemical reaction while the PVD only sprays a vaporized material on the substrate. One great advantage of CVD processing is that it can create coatings of uniform thickness even over complex shapes. For example, CVD can be used to uniformly coat carbon nanotubes with uniform rod size or even modify the CNT property. However, the limitation of this technique is the need of high temperature to activate chemical reaction, difficulty to mask surface, and the area of coating is limited by a reaction chamber.

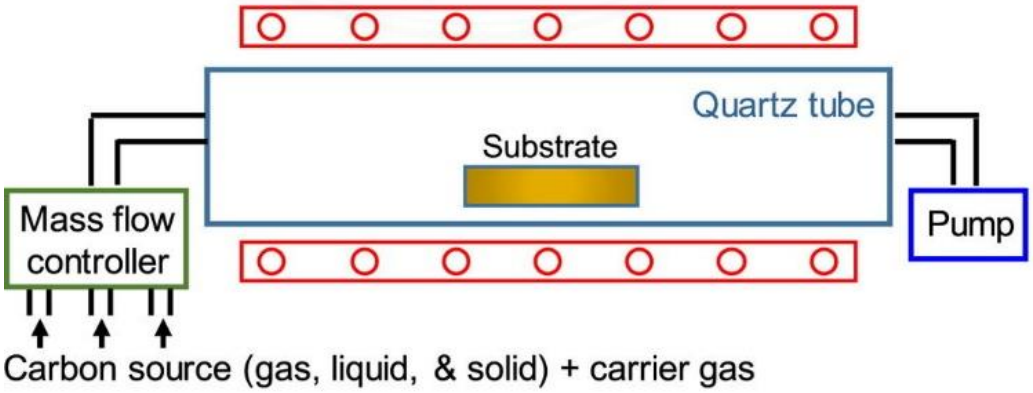

Figure 2.7 Chemical Vapor Deposition (CVD) system (Son & Ham, 2017)

Ref. code: 25655922300099OUH

For SERS application, CVD has been reported as a method for preparing 2D graphene for enhancing the Raman signal and to be utilized as a protective layer.

Federico et al.[ref] reported his work on preparing graphene by CVD and use it as a cover layer for AuNPs/ITO SERS substrate. They found that graphene helps promote the SERS signal and the AuNPs coverage are 6 folds better when there is graphene than without graphene.

Seiya Suzuki et al. (Nakabayashi et al., 2019) fabricated and tested the chemical stability of CVD graphene/AgNPs/SiO_2 SERS substate. They found that their SERS substrate can be used for enhancing the Raman signal of R6G even in concentrated hydrochloric acid or at temperatures up to 400 C. Thus, this chemical stability of SERS substate provides a new application such as molecular detections at high temperatures or in extreme acidic conditions.

M. EmreAyhan (Ayhan, 2020) also reported SERS activity of AgNPs@G nanocomposite SERS substrate prepared by AgNPs decorated on a CVD graphene surface. The value of the enhancement factor (EF) up to 7.2×10^4 suggests that the AgNPs@G nanostructure substrates have perfect SERS properties.

2.3.3.2 Electrophoretic deposition

Electrophoretic deposition (EPD) is a chemical coating process that uses an electric field to force a colloidal particle to migrate and deposit on a conductive substrate. Both alternating current (AC) and direct current (DC) electrical fields have been applied in the EPD process although DC fields are more common. The advantage of this deposition technique is the cost effectiveness, facile modification, high quality of nano/microstructure, and the controllable of shape, size, and thickness of particle. EPD could be anodic or cathodic electrophoretic deposition, depending on which electrode the deposition occurs. The electrophoretic setup is shown in Figure 2.8. The mechanisms of EPD are still not completely understood. It can be considered as a two-step process, first the particle migrates to the substrate due to an applied electric field. Particles will lose their charge at the electrode surface then they will aggregate and form a rigid solid layer on the substrate.

Ref. code: 25655922300099OUH

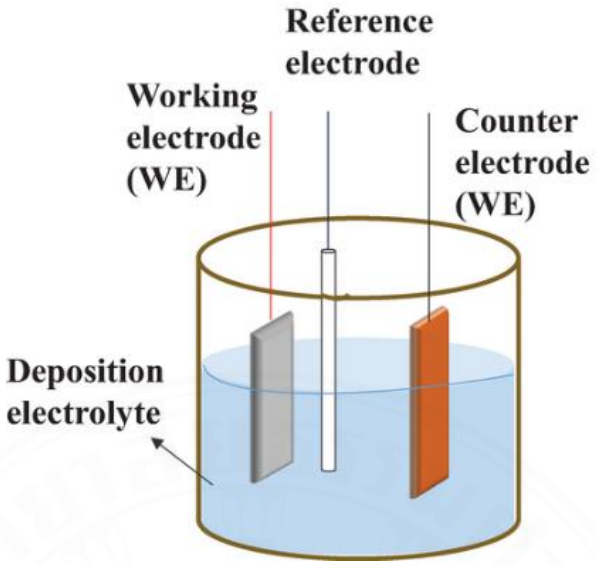

Figure 2.8 Electrophoretic deposition setup

Electrophoretic deposition is widely used for preparing metal nanoparticles for SERS substrates because it can produce a high quantity nanoparticle. Shape and size of nanoparticle fabricated by this technique can be tuned to adjust the hot spot for enhancing the Raman signal. The metal material prepared by this method for SERS application include Ag (Rivera-Rangel et al., 2020; Wang et al., 2019), Au (Choi et al., 2010; Zhu et al., 2021), Pt (Choi et al., 2010).

According to the variation of electrodeposition condition, several shapes of nanoparticle have been reported for SERS application, for example a ball like, flower like, and a leaf like shape. Those shapes, gaps, and different sizes strongly affect SERS performance (Jeon et al., 2013; Lal et al., 2008; Zhang et al., 2018). Thus, this fabrication method is a promising way to prepare SERS substrates that match our application.

2.4 Graphene for SERS application

Graphene is an allotrope of carbon in the form of a single layer of carbon atoms arranged in a hexagonal two-dimensional honeycomb lattice. Graphite is when graphene layers stack together with a van der Waal force. One way to produce graphene

Ref. code: 25655922300099OUH

is to exfoliate each graphene layer out of graphite, which is a top-down process. Another way to prepare graphene is a bottom-up process, for instance CVD. Graphene has unique physical, electrical, and mechanical properties that has attracted attention to be used in many applications. Graphene possesses many excellent properties that make it a promising material for SERS application. Its large surface area makes it good for molecular adsorption. Excellent charge transfer ability of graphene makes it to be a chemical enhancement material for SERS. Its photoluminescent quenching helps eliminate fluorescence background from the Raman signal. Moreover, graphene can be used as a protective layer for metal from oxidation which will improve the durability and stability of the SERS substrate. The examples of using graphene in SERS applications are shown below.

Jaehong Lee et al. (J. Lee et al., 2015) used graphene as an encapsulated layer on AgNps for oxidative resistance for SERS substrates. The AgNps was formed on a SiO_2 substrate then coated with PMMA which is used as a carbon source. The as prepared surface was thermally annealed resulting in a graphene layer coated on AgNPs. SERS performance was studied with R6G molecules, they found that their SERS substrate has a high stability while the performance still remains.

Lu Liu et al. (Liu et al., 2020) prepared multilayer silver nanoparticle hybrid graphene (AgNps/graphene) as a SERS substrate aiming to use the combination of chemical enhancement effect from graphene and electromagnetic enhancement from silver nanoparticles to enhance Raman signal. They found that their SERS substrate could be used to detect Raman signal on rhodamine 6G (R6G) and crystal violet at low concentration as 10^{-14} and 10^{-12} M, respectively.

Similar work reported by Xianwu Xiu et al. (Guo et al., 2018) using GO as a protective layer for SERS substrate. They fabricated a multilayer AgNP/graphene SERs substrate attempt to make a 3D SERs substrate with increasing hot spots. Studying the R6G Raman signal, they found that their SERs substrate can detect R6G at LOD of 10^{-12} M.

Ref. code: 25655922300099OUH

Another report of using GO as a protective layer for SERs substrate was reported by Kseniya et al. (Girel et al., 2018) They use GO coating on AgNPs layer and found that the intensity decayed due to the oxidized metal layer after 2 times.

Xiaodong Li (Li, 2018)reported the other role of graphene as a photoluminescent quenching. They studied the effect of graphene oxide (GO) deposit on AgNps layers to the SERS performance and found that GO helped reduce fluorescent background while measuring Raman signal of R6G. Moreover, he also reports that the oxygen group plays an important role in promoting SERS effects which he suggests that by understanding of the effect of oxygen number to SERS process, the SERS performance could be controlled.

2.5 Flexible SERS

Most of the commonly used SERS substrates rely on a rigid glass slide or silicon which limits their usage in the real-world applications. Thus, developing a flexible SERS substrate has been of interest to many researchers. When preparing a flexible SERS substrate, several requirements should be satisfied including ease of fabrication, low cost, high sensitivity, and reproducibility. Several materials were proposed to be used as the flexible SERS substrate, for example PDMS (Novara et al., 2016), PMMA (Zhong et al., 2014), and adhesive tape (Guo et al., 2019). Hengwei Qiu et al. (Qiu et al., 2017) proposed the flexible SERS based Ag-nanoflowers/PMMA as a high-performance SERS substrate using the chemical reduction and spin coating process. Their sensor could detect rhodamine 6G at concentrations as low as 10^{-14} M. Pawan Kumar et al. (Kumar et al., 2017) have demonstrated another type of a SERS substrate prepared by evaporating Ag on a patterned PDMS surface and could be used as a high sensitivity sensor. Jiaolai jiang et al. (Jiang et al., 2018) reported on the tape-wrapped SERS technique that used adhesive tape to transfer the target molecule of the sample before measuring the Raman signal on the silver nanorod fabricated by the atomic layer deposition (ALD) method. Nevertheless, those indirect detection techniques are either short storage life or difficult to fabricate. Accordingly, in this work, we propose the

Ref. code: 25655922300099OUH

facile fabrication of a long shelf-life polymer-based SERS substrate based on graphene/Ag/polymer (G/Ag/Polymer).

2.6 Summary

Film-based SERS substrates have greatly attracted attention recently due to its stability and repeatability and convenience to be used for a field test. However, due to oxidation of noble metals on the surface, a coating or special packaging step is required to overcome those problems. Thus, increase the price of the SERS fabrication and sometime lower SERS performance. Graphene is a 2D material that has excellent optical, chemical, and electrical properties that could be used for SERS applications. In this work, a hybrid material of G/Ag/Polymer is proposed to be used as a SERS substrate for chemical detection. Silver nanoparticle as an enhancement material was prepare by electrophoretic deposition. The effect of current density and deposition time on the silver nanostructure and Raman signal enhancement was also investigated. Graphene was prepared by Chemical vapor deposition technique. Graphene functions as a protective layer of the SERS substrate and assist enhance Raman signal via chemical enhancement. Graphene decorated silver nanoparticle was transfer on a polymer for using as a supporting material for SERs substrate. The performance of the SERS substrate including the homogeneity, sensitivity, and stability were systematically examined. Due to the transparency and flexibility of the tape-based sensor, it could be attached directly on the sample, and the SERS signal could be collected without taking the sensor off the sample. Thus, this propose SERS substrate could be a great promise to use for field testing.

Ref. code: 25655922300099OUH

CHAPTER 3
METHODOLOGY

3.1 Preparation of flexible SERS substrate

The preparation of a flexible SERS substrate consists of four steps as shown in Figure 3.1. First, graphene was prepared on copper foil by chemical vapor deposition (CVD), then silver nanoparticles were electrodeposited on graphene/copper. Next, that prepared substrate was transferred onto a polymer layer, and the copper was then removed by chemical etching. The final flexible SERS substrate structure consists of the silver nanoparticle layer sandwiched between the protective graphene and the polymer layers (G/Ag/polymer).

The ideal polymer for SERS substrates should be transparent to allow excited laser light to pass through, less fluorescence to avoid high background signal and no Raman signal at the same wave number with an analyte. Silver nanoparticles used as the metal for enhancing the Raman signal should have a uniform size, gap and distribution on the substrate to provide high SERS performance, uniformity, repeatability, and reproducibility for the SERS sensor. Graphene should cover all of the substrate evenly to help prevent oxidation of silver nanoparticles and assist Raman signal amplification through a chemical enhancement.

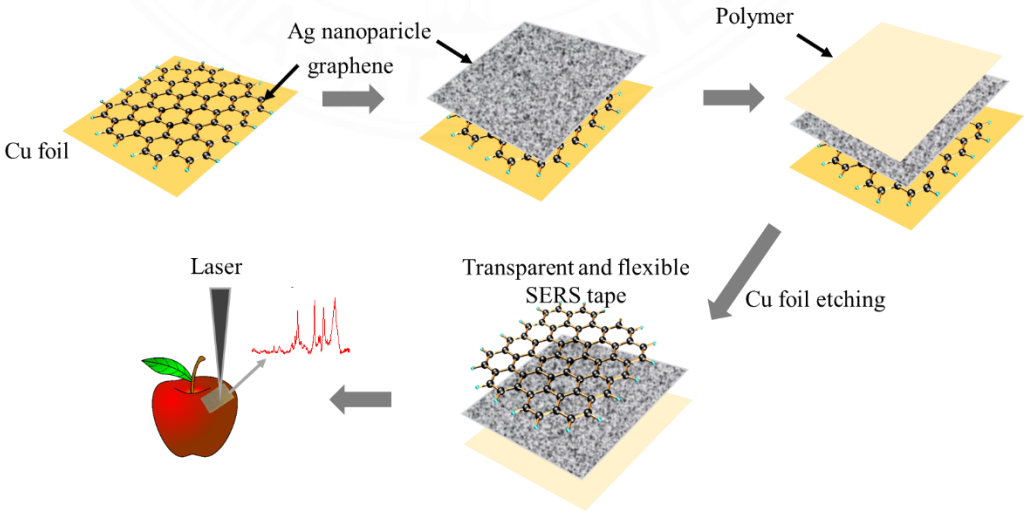

Figure 3.1 Schematic illustration of the process for the fabrication of the G/AgNPs/Polymer substrate and the potential use of the developed substrate.

Ref. code: 25655922300099OUH

3.1.1 Preparation of graphene on a copper foil substrate

The graphene sheet was grown by the chemical vapor deposition (CVD) technique onto a copper foil substrate. Copper foil was cut into 11 x 20 cm^2 sheets and ultrasonically cleaned in ethanol for 10 min and dried under flow nitrogen. Copper foil was then loaded into the quartz tube of the CVD machine (Planar TECH, planarGlow-6E) and graphene was grown with methane as a carbon source and hydrogen as a gas carrier. The growth condition was performed at the pressure of 5 Torr with 60 sccm methane and 200 sccm hydrogen at 1000 ^oC for 30 minutes.

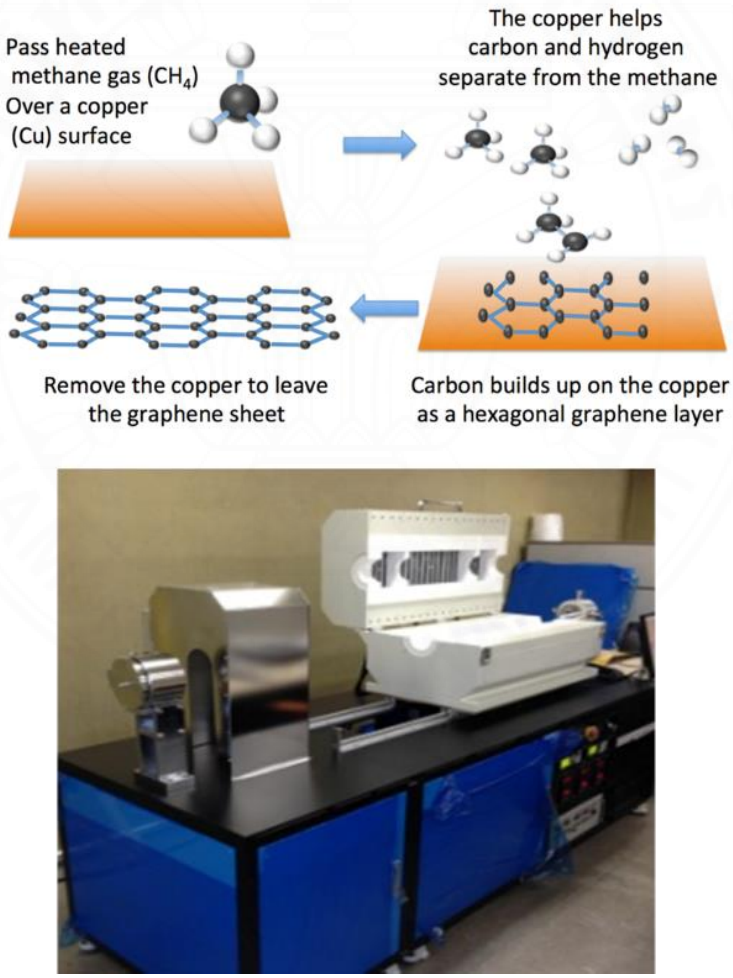

Figure 3.2 Mechanism of growing graphene on the copper substrate (top) and the CVD system used for growing graphene in this work (bottom)

Ref. code: 25655922300099OUH

Figure 3.2 depicts the mechanism of growing graphene on copper foil and the CVD system used in this work. The copper acts as catalyst to catalyze the dehydrogenation of the methane adsorbed on the copper surface, leaving carbon to form graphene on the copper foil surface. The presence of graphene was confirmed using Raman spectroscopy.

3.1.2 Electrodeposition of silver nanoparticles on graphene

The prepared graphene was subsequently used as a substrate for electrodeposition of silver nanoparticles (Ag). The electrodeposition was performed in the mixture of 10 mM silver nitrate (sigma Aldrich, 99%) and 60 mM citric acid (sigma Aldrich, 99.5%) electrolyte using potentiostat (Metrohm, Autolab PGSTAT302N) in a three-electrode system. Silver nitrate acts as a silver source while the citrate ions play multiple roles in the synthesis process, including as a reducing agent, a stabilizer, and a particle shape-control.

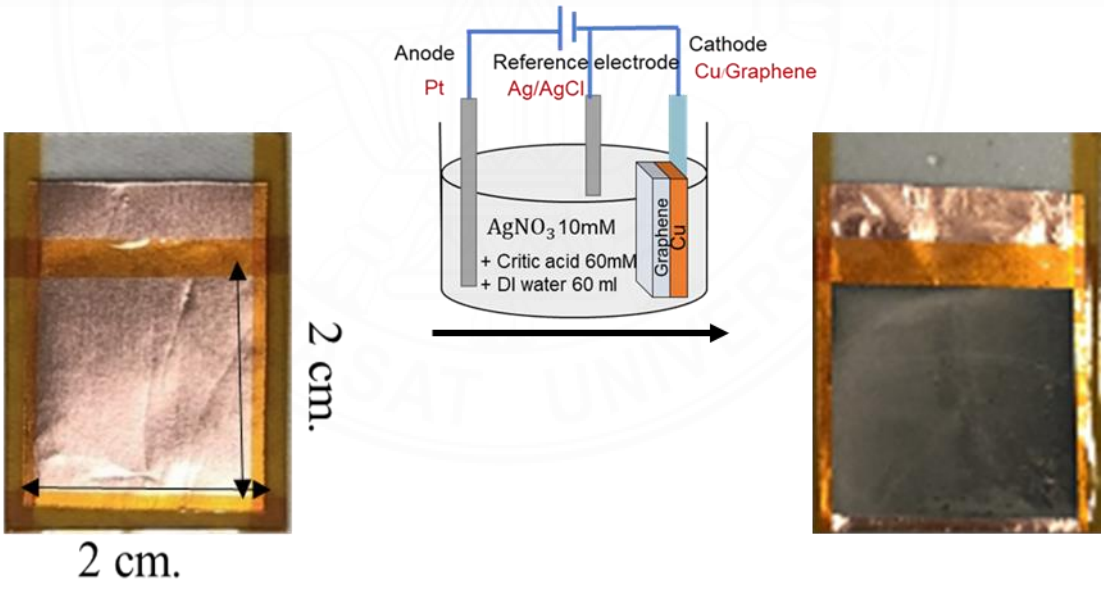

Figure 3.3 Electrodeposition of silver nanoparticles onto graphene/Cu substrate. Image on the left is the graphene/Cu before electrodeposition. Image on the right is after electrodeposition showing the deposited the silver layer deposited on the surface of the graphene/Cu substrate.

Ref. code: 25655922300099OUH

The current density and deposition time was optimized to find a suitable morphology of silver nanoparticles for Raman enhancement. The setup for electrodeposition is shown in Figure 3.3. Graphene on a copper substrate was used as a working electrode. Platinum rod and the Ag/AgCl electrode were used as a counter and a reference electrode, respectively. Current density and time for electrodeposition was varied to get the best Raman enhancement.

3.1.3 Preparation of polymer protective layer onto the Ag-decorated graphene

There are two types of protective polymers used in this research: polydimethylsiloxane (PDMS) and polyimide tape (PI). Figure 3.4 shows the picture of PDMS that consists of an elastomer base and a curing agent (left) and polyimide tape (right).

Figure 3.4 The PDMS precursor together with its curing agent (left) and the polyimide tape used in this work (right)

3.1.3.1 PDMS coating

PDMS is a polymer that is widely used for fabricating micro and nano-devices. It is chemically inert, has high thermal stability, and is optically transparent. These properties are excellent for use as a SERS substrate because it can withstand the etching solution in the SERS fabricating process. Additionally, its optical transparent properties will allow the excitation and scattering light to pass through the SERS substrate to the optical system of the Raman machine.

Ref. code: 25655922300099OUH

In order to prepare the PDMS layer, spin coating was used because it's suitable for liquid coating to provide a uniform and adjustable thickness of the PDMS layer. The ideal thickness of PDMS must possess the low absorption of the laser source, be robust and easy to handle. Once silver nanoparticles were decorated onto the graphene/Cu, the sample was then immediately coated with PDMS premixed with curing agent. PDMS was prepared by mixing the polymer base and curing agent at the ratio of 10:1 and degassing to remove all the bubbles. Then the prepared Ag/graphene/Cu was coated with PDMS using a spin coater (Polos, Spin200i) at 300 rpm for 60 s and left to cure at 80 ^{o}C for 1 h. The PDMS/Ag/graphene/Cu, or PDMS/Ag/Cu substrate was then placed in 40 mg/ml of $FeCl_3$ for 2 h to remove the copper and obtain the G/Ag/PDMS SERS substrate.

3.1.3.2 Polyimide tape

Polyimide tape is flexible, transparent, biocompatible, and has high tensile strength. It has a thermal stability, good chemical resistance, and excellent mechanical properties. Therefore, it is one of the good choices for a SERS substrate. Polyimide tape was mechanically pressed on the Ag/graphene/Cu then it was heated at 80 ^{o}C for 15 min before removing the copper layer in 40 mg/ml of $FeCl_3$ for 1.5 h to get the tape-based SERS substrate which consists of a G/Ag/PI structure.

The sucessfuly fabricaed of PDMS and PI SERS substrate are shown in Figure 3.5 (left) and (right), respectively.

Ref. code: 25655922300099OUH

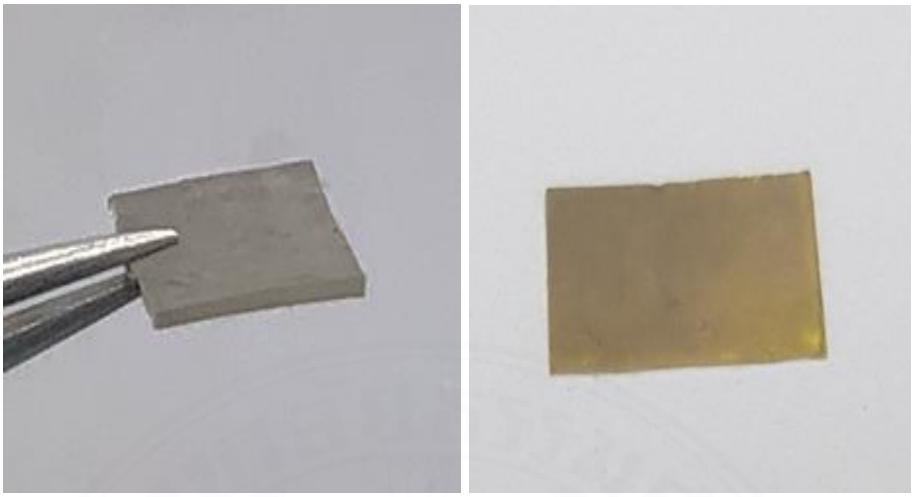

Figure 3.5 Picture of G/Ag/PDMS SERS substrate (left) and G/Ag/PI SERS substrate (right)

3.2 Characterizations

X-ray diffraction (XRD) is a nondestructive analytical technique for elemental and phase analysis of material. It also provides other structural parameters such as average grain size, crystallinity, and crystal defects. XRD consist of three basic elements: an X-ray tube, a sample holder, and an X-ray detector. X-rays generated by a cathode ray tube is direct through the optical system toward the sample. At the conditions that satisfy Bragg's law ($n\lambda=2d \sin \theta$) the diffracted X-rays can be detected, processed, and counted. In this work, an X-ray diffractometer (XRD: PANalytical) was used for characterizing the molecular structure of the prepared SERS substrate. The Ag decorated graphene on copper substrate was used for XRD characterization. The data were recorded using a Cu Kα X-ray source over a 10-90^{o} 2θ range with a counting time 0.5 step s^{-1} at step size of 0.02^{o}.

A Universal Testing Machine (UTM) (AGXV, SHIMADZU) was used for examining the mechanical properties of the SERS substrate. The effect of preparing PI-SERS substrate to the mechanical properties including tensile strength and elongation at break was investigated and compared with a bare PI substrate. Unfortunately testing with the PDMS SERS substrate cannot be performed due to the limitation of the device

Ref. code: 25655922300099OUH

fabrication. These tests were performed with a 10 KN load cell and a stroke length of 500 mm/min at room temperature and with a humidity of 50%.

SEM is a surface analysis technique that used a focused beam of electrons to scan over the sample surface. The electrons interact with atoms in the sample and will produce various signals that contain information about the surface topography and composition of the sample. In this work, FE-SEM and EDX (Hitachi, SU8030) analysis of SERS substrate was performed with the accelerating voltage at 10 kV and 8.0 mm working distance.

Raman spectroscopy is a vibrational sensitive technique for detecting inelastic scattering that causes a frequency shift from the incident light. The frequency shift relates to molecular vibration that can be used to identify the molecules. In this work, the Raman spectroscopy technique was used for determining graphene quality and detecting methyl parathion on the SERS substrate. Raman spectrometer (Renishaw, InVia Qontor) with the excitation energy and spot of laser were 0.48 mW and 1 μm, respectively was used throughout the experiment. The diffraction grid was set as 600 gr/mm and the integration time was set as 8 s. The laser light was coupled through an objective lens of 50×. A laser source at 785 nm was used for graphene analysis. While for the SERS measurement, a suitable laser source will be selected to obtain a high Raman signal and low interference signal from the substrate.

3.3 Study of the SERS performance

In order to determine the sensitivity of the SERS sensor, methyl parathion in ethanol was prepared in the concentration range from 2.5×10^{-5} M to 1×10^{-3} M. The molecular structure of methyl parathion is shown in Figure 3.6. The SERS substrate was cut into a dimension of 2x2 cm^2, then the primary peak at 1344 cm^{-1} was used for examining the Raman intensity.

Ref. code: 25655922300099OUH

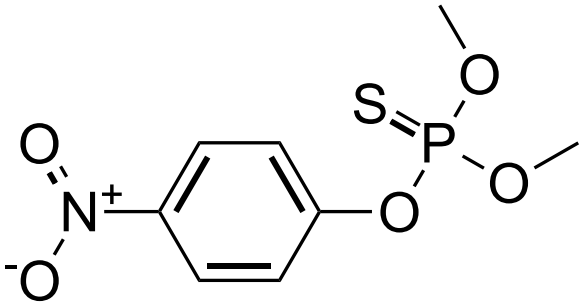

Figure 3.6 molecular structure of methyl parathion
(https://commons.wikimedia.org/w/index.php?curid=4291405)

3.4 Data pre-processing and analysis of Raman spectrum

The SERS enhancement factor (EF) is one of the most important parameters for characterizing the ability of a given substrate to enhance the Raman signal for SERS applications. It is calculated as follows:

$$\mathrm{EF} = \frac{I_{\mathrm{SERS}} / N_{\mathrm{SERS}}}{I_{\mathrm{bulk}} / N_{\mathrm{bulk}}} \tag{3.1}$$

where I_{SERS} is a SERS intensity and and I_{Bulk} is a Raman intensity of sample. N_{SERS} and N_{bulk} are the number of probed molecules on the SERS substrate and in the aqueous sample, respectively.

N_{bulk} was calculated based on the known volume and concentration of probed molecules dried on the substrate with known area compared those in the area under the excitation laser. The number of molecules drop on substrate is calculated as follows:

$$N_a = v \times c \times N_A \tag{3.2}$$

Where N_a is a number of molecules drop on area a, v is a volume of analyte, and N_A is the Avogadro number.

Since only the molecule under excitation laser is contribute to Raman signal. The laser spot area is calculated by

Ref. code: 25655922300099OUH

$$A = \pi r^2 \tag{3.3}$$

Where r is a radius of laser which was estimated by:

$$r = \frac{1}{2}\left(\frac{1.22\lambda}{Numerical\ Aperture}\right) \tag{3.4}$$

Then the N_{bulk} is calculate by compared the number of molecules drop on area a in equation (2) to the number of molecules in laser spot area.

To calculate the number of SERS probe N_{SERS}, only the molecules that involve in SERS process will be considered. It was estimated by assuming that only molecule locates within the gap between metal nanoparticle involve the SERS process. Thus, it can be estimated by dividing the whole laser spot area by the size of analyte molecule.

$$N_{SERS} = \frac{Area\ of\ laser\ spot}{size\ of\ molecule} \tag{3.5}$$

The detailed calculations based on this formula is shown in the appendix.

The Raman spectra of hybrid material generally have high complexity because they contain numerous numbers of peaks with different intensities and forms. In order to compare a large set of spectra, data pre-processing is necessary to reduce the irrelevant systematic variation in the spectra to improve the accuracy for data analysis. The basic data pre-processing includes background correction, smoothing, and normalization etc. In this work, all the collected data was pre-processed by background removal to eliminate the fluorescence signal. To compare the intensity between data set, the data was normalized by its mean and extended multiplicative signal correction (EMSC) was used to eliminate the scattering effects from the sample.

Ref. code: 25655922300099OUH

CHAPTER 4
RESULTS AND DISCUSSION

4.1 Characterizations of graphene/copper foil substrate

Quality graphene prepared by CVD on copper foil was verified by Raman spectroscopy. Raman spectra of graphene showing the D, G and 2D peak is shown in Figure 4.1, The D band appeared at ~1332 cm^{-1}, the G band appeared at 1573 cm^{-1}, and 2D peak at 2700 cm^{-1}. The G peak corresponds to the E2g phonon at the Brillouin zone center. The D peak is attributed to the amount of disorders or defects. The second order of the zone boundary phonons gives rise to the 2D peak and it appears as a strong single peak in monolayer graphene. The 2D band appearance can be used to distinguish the graphene from graphite. It is known that the I_{2D}/I_G ratio depends on the number of graphene layers (Reina et al., 2009). The ratio $I_{2D}/I_G \sim 2–3$ is for monolayer graphene, $2 > I_{2D}/I_G > 1$ for bilayer graphene and $I_{2D}/I_G < 1$ for multilayer graphene. The intensity ratio of the 2D to the G band (I_{2D}/I_G) of our prepared graphene is 2.2 which indicates a few layers of graphene.

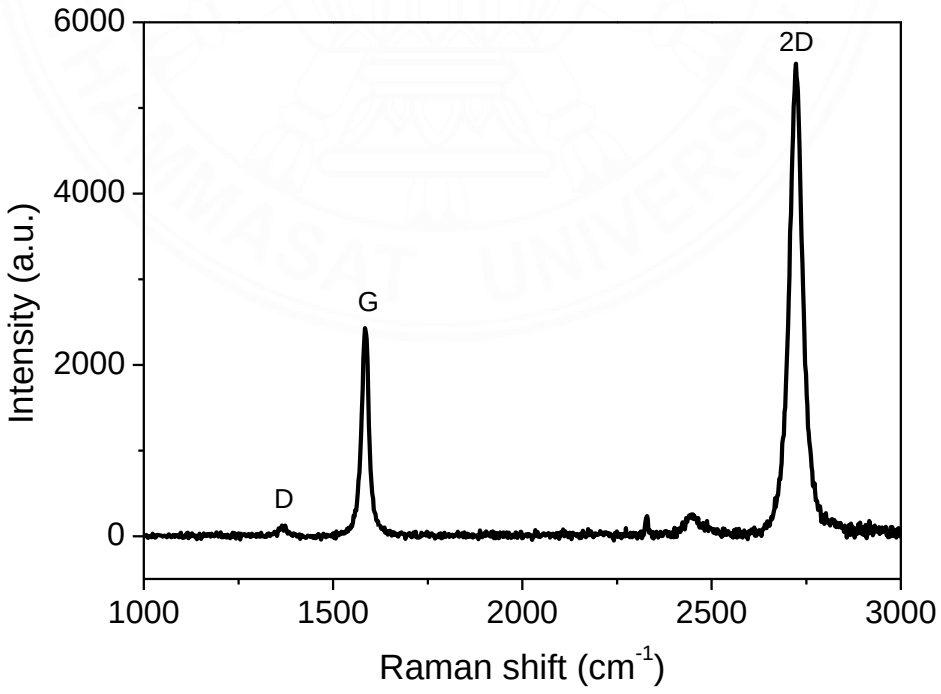

Figure 4.1 Raman spectra of graphene on copper foil

Ref. code: 25655922300099OUH

The XRD patterns of silver decorated on graphene/Cu is shown in Figure 4.2. It exhibits sharp peaks of silver at 38.1°, 44.3°, 64.4° and 77.5° and characteristic peaks from copper at 43.1°, 50.5° and 74.1°. The sharp diffraction peaks indicate the crystalline characteristic of both Cu and Ag. There are no evident graphene peaks shown in XRD due to the lack of crystalline order in the graphene structure. Therefore, it could be confirmed that a high crystallinity silver can be obtained by electrophoretic deposition.

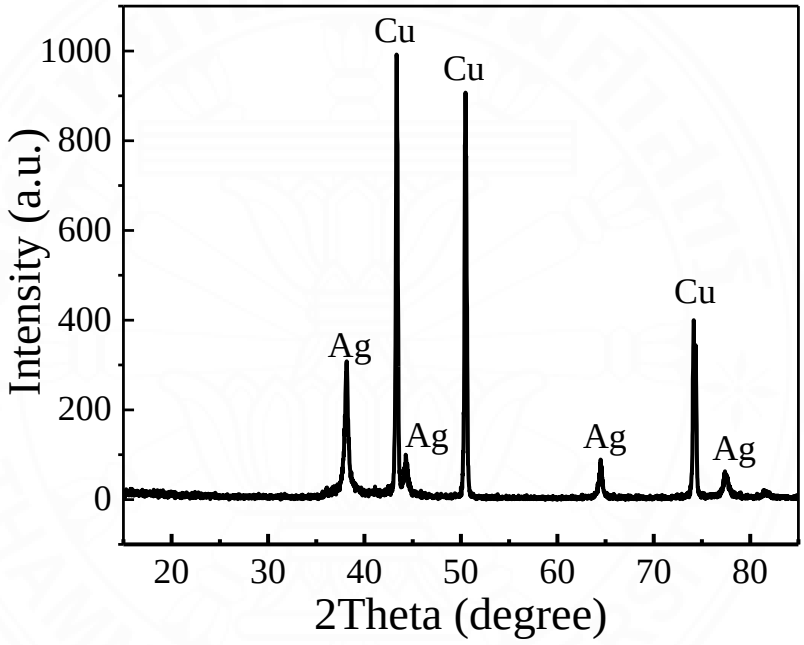

Figure 4.2 XRD pattern of silver prepared by electrodeposition technique.

Ref. code: 25655922300099OUH

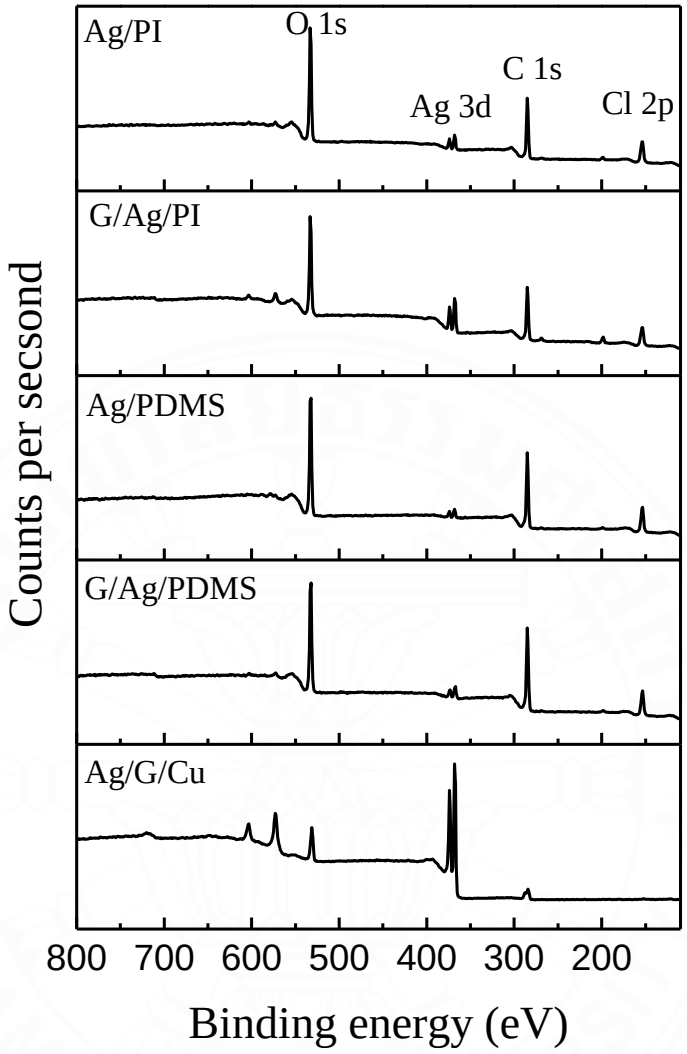

(a)

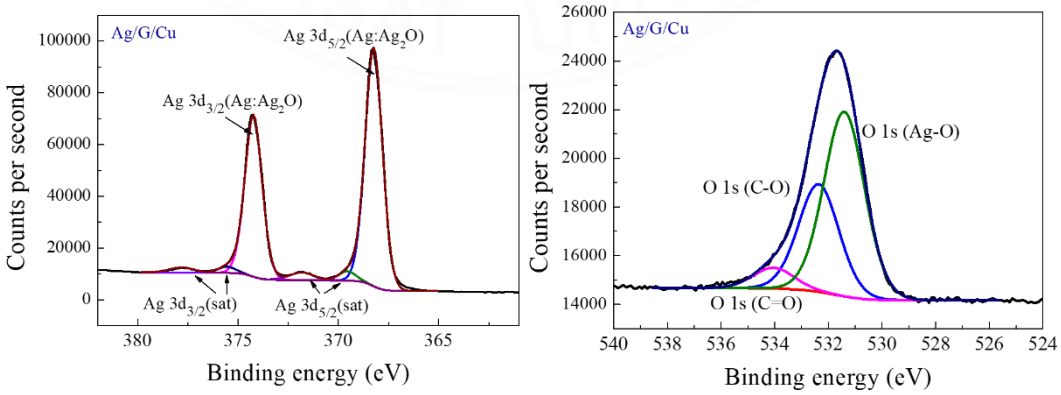

(b)

Ref. code: 25655922300099OUH

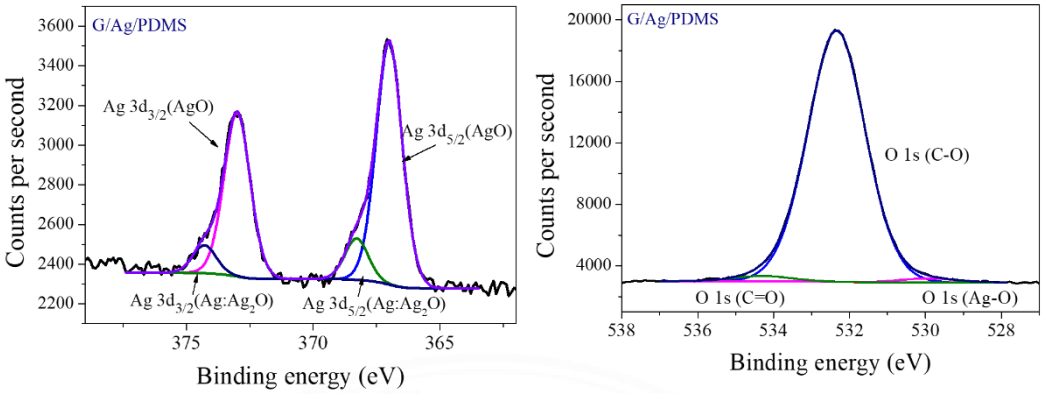
G/Ag/PDMS
Ag 3d3/2(AgO)
Ag 3d5/2(AgO)
Ag 3d3/2(Ag:Ag2O)
Ag 3d5/2(Ag:Ag2O)
Counts per second
Binding energy (eV)
G/Ag/PDMS
O 1s (C-O)
O 1s (C=O)
O 1s (Ag-O)
Counts per second
Binding energy (eV)

(c)

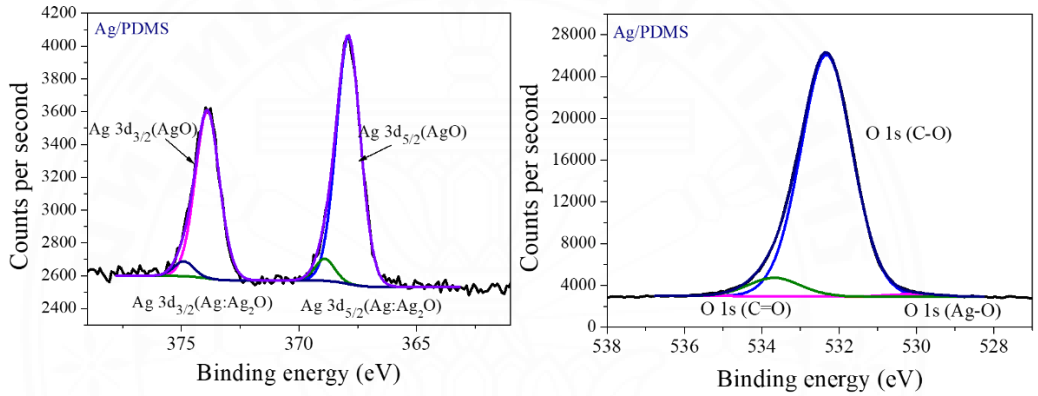
Ag/PDMS
Ag 3d3/2(AgO)
Ag 3d5/2(AgO)
Ag 3d3/2(Ag:Ag2O)
Ag 3d5/2(Ag:Ag2O)
Counts per second
Binding energy (eV)
Ag/PDMS
O 1s (C-O)
O 1s (C=O)
O 1s (Ag-O)
Counts per second
Binding energy (eV)

(d)

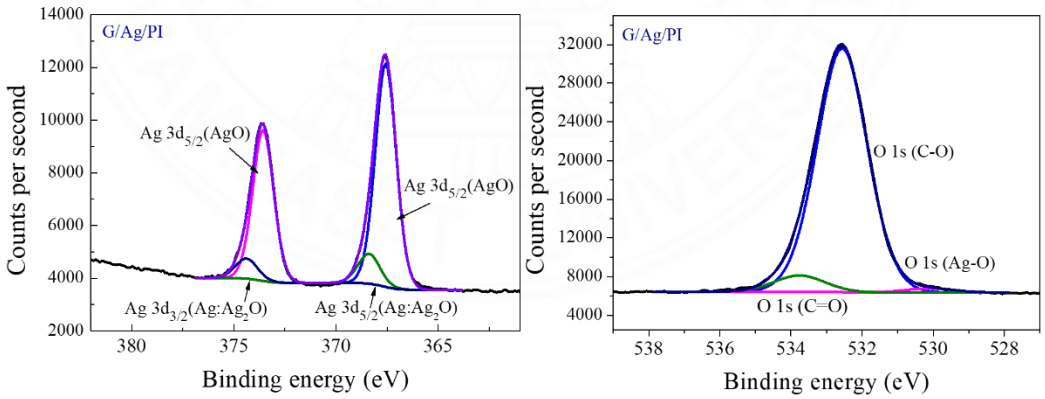
G/Ag/PI
Ag 3d5/2(AgO)
Ag 3d5/2(AgO)
Ag 3d3/2(Ag:Ag2O)
Ag 3d5/2(Ag:Ag2O)
Counts per second
Binding energy (eV)
G/Ag/PI
O 1s (C-O)
O 1s (Ag-O)
O 1s (C=O)
Counts per second
Binding energy (eV)

(e)

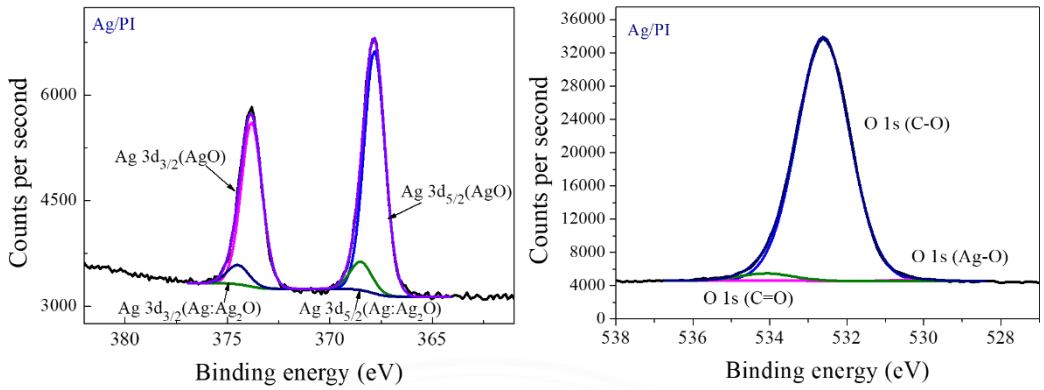

(f)

Figure 4.3 The wide scan of XPS spectra (a) and the detailed scan of Ag 3d and O 1s component of Ag/G/Cu (b), G/Ag/PDMS(c), Ag/PDMS (d), G/Ag/PI(e) and Ag/PI (f)

X-ray photoelectron spectroscopy (XPS) analysis was used to investigate the quality of silver and the effect of graphene coverage on a SERS substrate. The ability of graphene for protecting silver from oxidation was determined by surveying the chemical state of metallic silver and its oxides. Figure 4.3(a) shows the wide scan XPS spectra of AgNPs/G/Cu, G/AgNPs/PI and AgNPs/PI. All the XPS spectra show the presence of silver, oxygen, and carbon, while a little Cl appears in the PI SERS substrates which could be due to contamination from the etching process. Detailed scans of the Ag 3d and O 1s region were recorded to define the chemical state of silver and oxygen in each sample and are shown in Figure 4.3 (b-f). The O 1s spectrum from all samples show multi chemical states of oxygen due to AgO, ether carbon (C-O) and carbonyl carbon (C=O). For the silver deposited on Cu/G, we found the combination of Ag 3d(Ag:Ag_2O) spectra peak at 368.2 eV and satellite peak which is attributed to the metallic silver (Firet et al., 2019). While the samples that were transferred on PI tape show the additional Ag 3d (AgO) spectra and the disappearance of the satellite peak infers the oxidation of the sample. The formation of AgO was compared by considering the Ag 3d (AgO)/ Ag 3d (Ag:Ag_2O) ratio for each sample and is shown in table 4.1. It shows that the Ag/G/Cu have the highest Ag:Ag_2O content and no evidence of AgO component. While other samples that undergo the etching process show less Ag/Ag_2O content and a high AgO content. However, comparing between the samples with and without graphene coverage, it shows that the one with a graphene protected

Ref. code: 25655922300099OUH

layer provides lower AgO formation on the surface. Thus, the prepared sample was oxidized during the etching process and graphene could help protect against oxidation from occurring.

Table 4.1 Comparison of atomic concentration of silver phase of each SERS substrate

Quantification	Atomic conc. [%]* Only consider Ag and O		
	AgNPs/G/Cu	G/AgNPs/PI	AgNPs/PI
Ag $3d_{5/2}$ (Ag:Ag_2O)	27.36	0.40	0.13
Ag $3d_{3/2}$ (Ag:Ag_2O)	18.52	0.27	0.09
Ag $3d_{5/2}$ (AgO)	-	2.82	1.10
Ag $3d_{3/2}$ (AgO)	-	1.91	0.74
Ratio Ag using $3d_{5/2}$ (AgO)/(Ag:Ag_2O)	-	7.05	8.50
Ratio Ag using $3d_{3/2}$ (AgO)/(Ag:Ag_2O)	-	7.07	8.22

Graphene coverage on a sample is another crucial thing of concern because it is a protective layer for metals which help extend the shelf life of SERS substrates. The existence of graphene on PDMS and PI SERS substrates was investigated by performing the Raman mapping measurement on 9 areas of the 1x1 cm^2 SERS substrate. The 785 nm excitation laser source was scanned over the area of 600 x 500 μm^2 with 10 um steps size. The intensity plot of the G band of graphene (1582 cm^{-1}) on each map was measured as shown in Figure 4.4 (a) and (b) for PDMS and SERS substrate, respectively. The various colors of the map indicate the Raman intensity of the G band. The results show that, a similar mapping profile was found from every area on the substrate which indicate that graphene was transferred and covered the entire area of the PDMS and PI substrate. Comparing between the two types of SERS substrates, it appears that PI SERS substrate provides more variation of color on each map than that in the PDMS SERS substrate. This implies that transferring graphene onto PDMS covers more evenly on the substrate than that on the PI substrate.

Ref. code: 25655922300099OUH

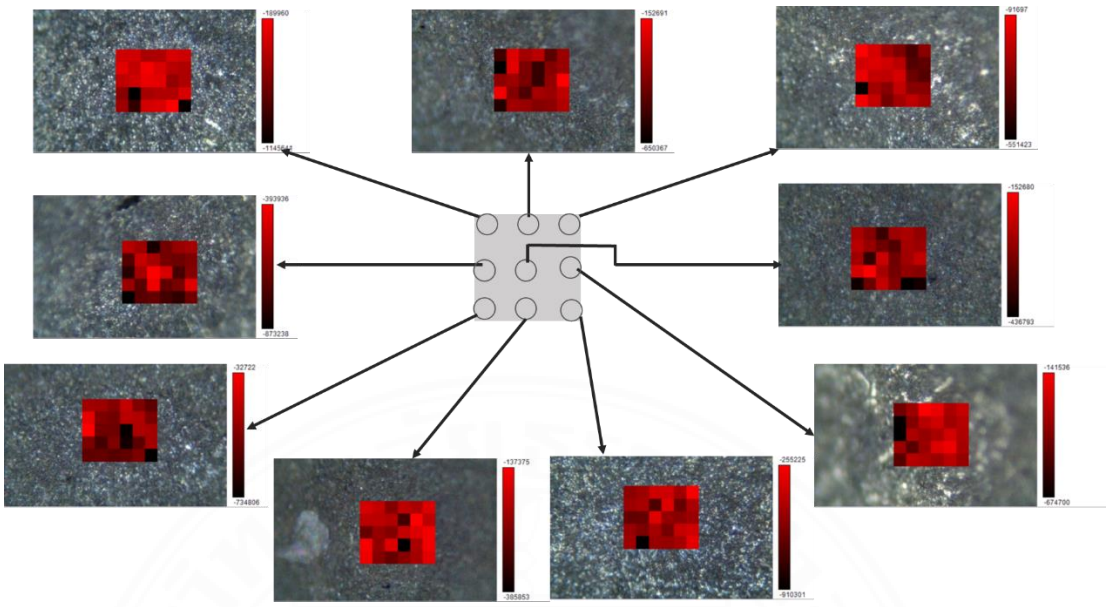

(a)

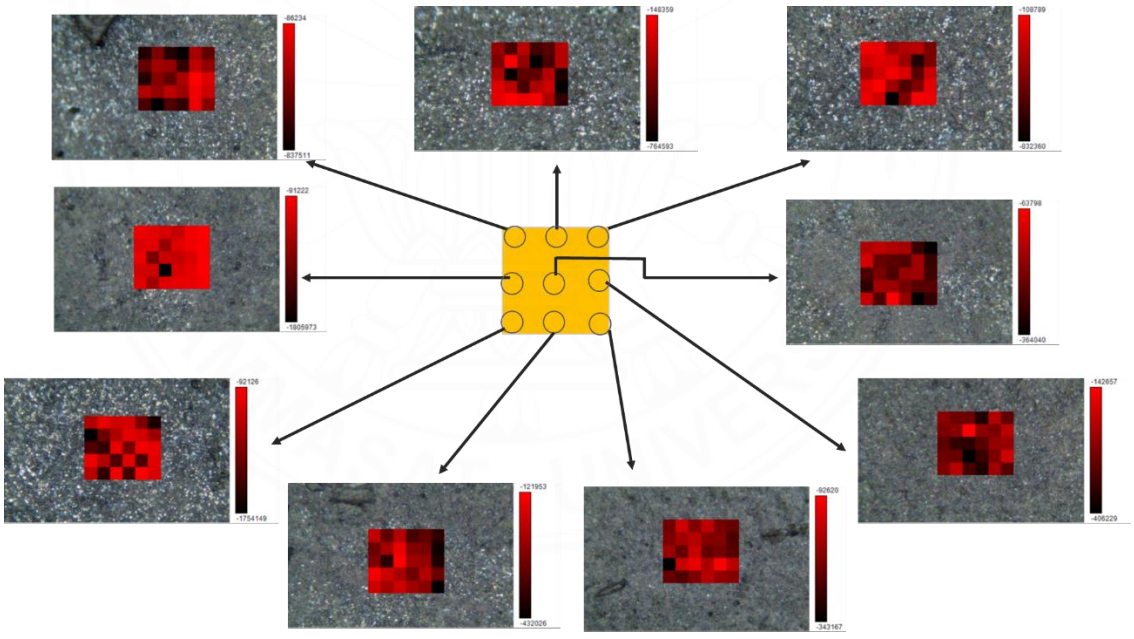

(b)

Figure 4.4 The intensity mapping plot of the G band (1582 cm^{-1}) of graphene performed on PDMS (a) and PI (b) SERS substrate

Ref. code: 25655922300099OUH

4.2 Effect of current density and deposition time to silver nanoparticle morphology.

SEM was used for examining the morphology and mechanism of silver nanoparticle growth on the graphene/Cu surface. Figure 4.5 shows the image of the silver nanoparticles from electrodeposition at different current densities. The rattan ball-shaped silver nanoparticles were found uniformly dispersed over the surface of substrate area. The sizes of the silver nanoparticles are about 1.2-1.6 μm for the applied current density 1, 5, and 10 μAcm^{-2} and in the range 1.8-2.0 μm for the applied current density of 20, 50, and 100 μAcm^{-2}. The rattan ball-shape of the silver nanoparticles at different current densities are quite similar, the gap between the strands within the rattan ball is found to be in the range 30-100 nm and is not affected by the current density.

However, the gap between silver nanoparticles is quite different at different current densities. At low current density of 1 μAcm^{-2}, the distance between silver nanoparticles is in the range 0.6-1.6 μm. This is because there is less potential to start the reaction so fewer seed particles for generating silver nanoparticle clusters. At the current density at 5-20 μAcm^{-2}, there are more forces to push the reaction so there are more Ag seeds to nucleate the silver nanoparticles. Consequently, the gaps between the silver nanoparticles are in the range 0.5-1 μm. However, at a high current density from 50-100 μAcm^{-2} the gap between them becomes large again (about 1.2-1.8 μm) which might be the results of hydrogen evolution at high current density (Lee et al., 2018). Those effect leading to the decreasing of an effective area for growing silver nanoparticle.

Ref. code: 25655922300099OUH

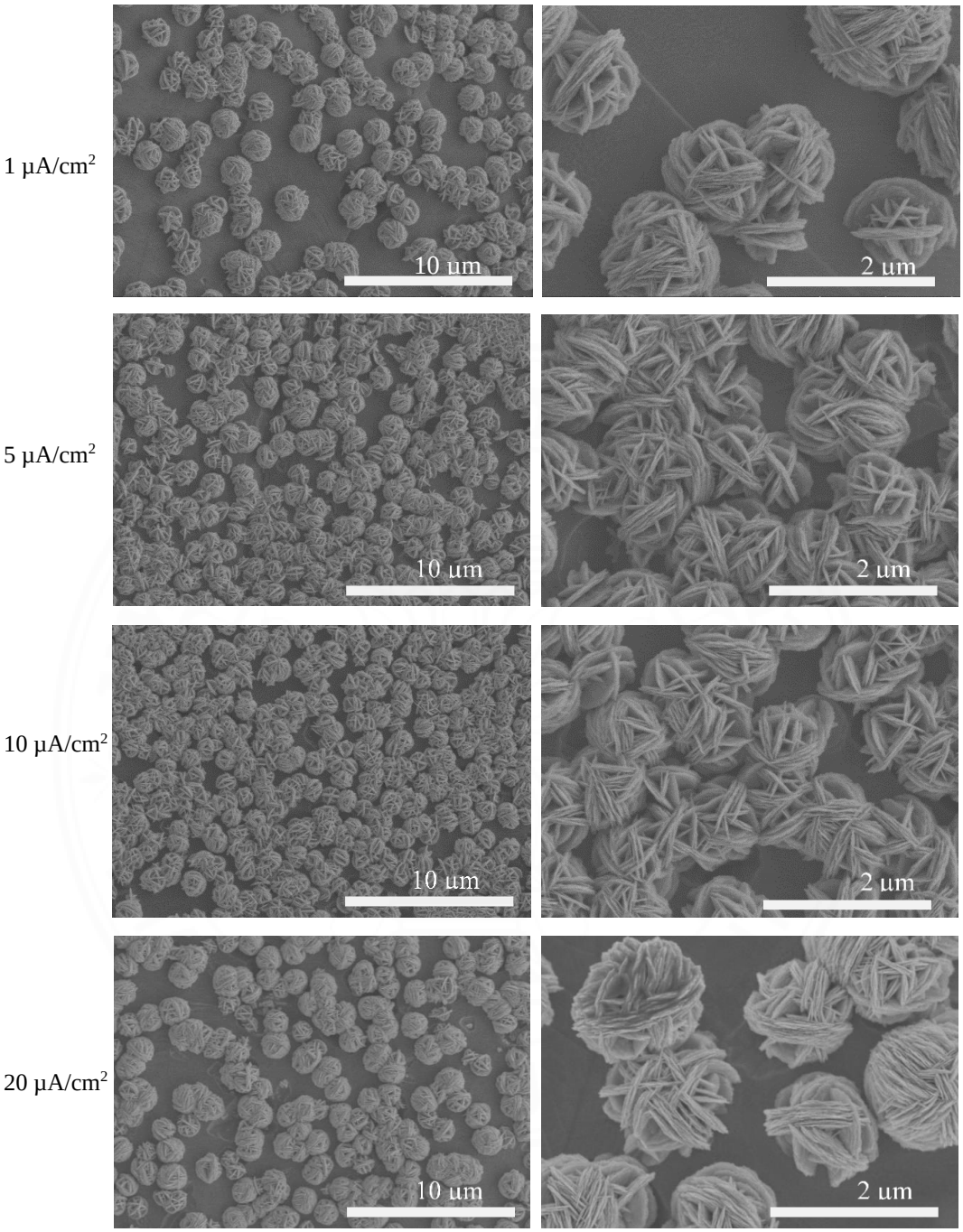
1 μA/cm²
10 μm
2 μm
5 μA/cm²
10 μm
2 μm
10 μA/cm²
10 μm
2 μm
20 μA/cm²
10 μm
2 μm

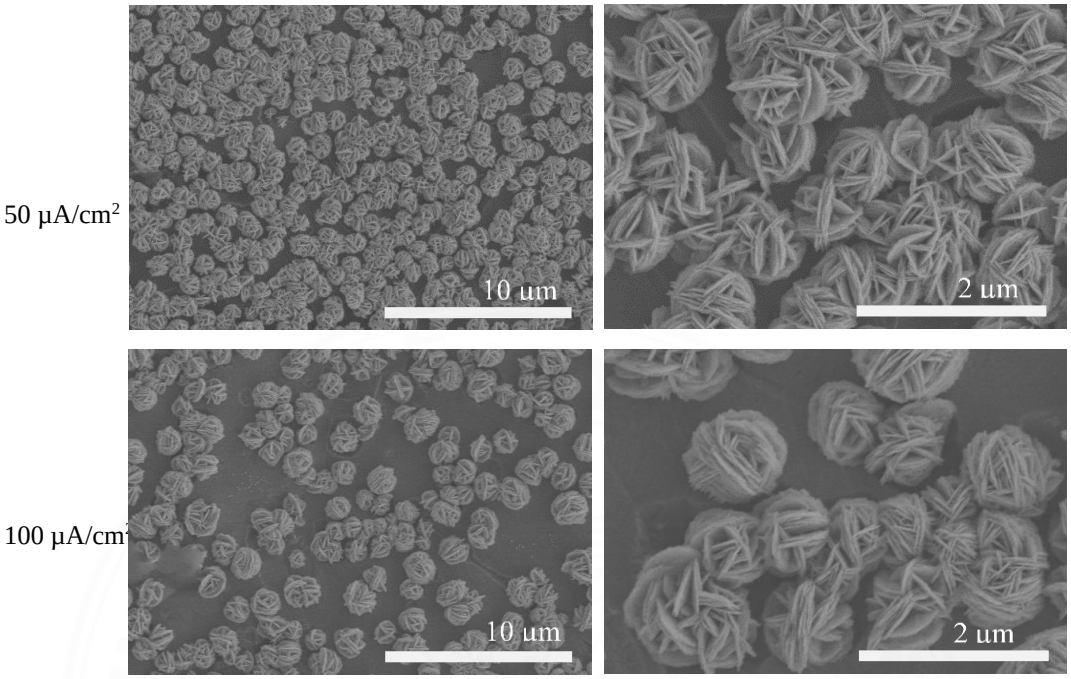

Figure 4.5 FE-SEM images of silver nanoparticle prepared by the electrodeposition method at current densities of 1, 5, 10, 20, 50, 100 μA/cm^2 for 180 s on a graphene/Cu substrate.

Next, the morphology of the silver nanoparticles generated at a fixed current density of 10 μA/cm^2 with various deposition times is shown in Figure 4.6. It can be observed that the distribution of silver particles is similar throughout, but the particles grew larger with longer deposition time. Hence, it may be assumed that the current density affects the initial distribution of the nanoparticles, while the deposition time affects the size of the nanoparticle cluster.

Ref. code: 25655922300099OUH

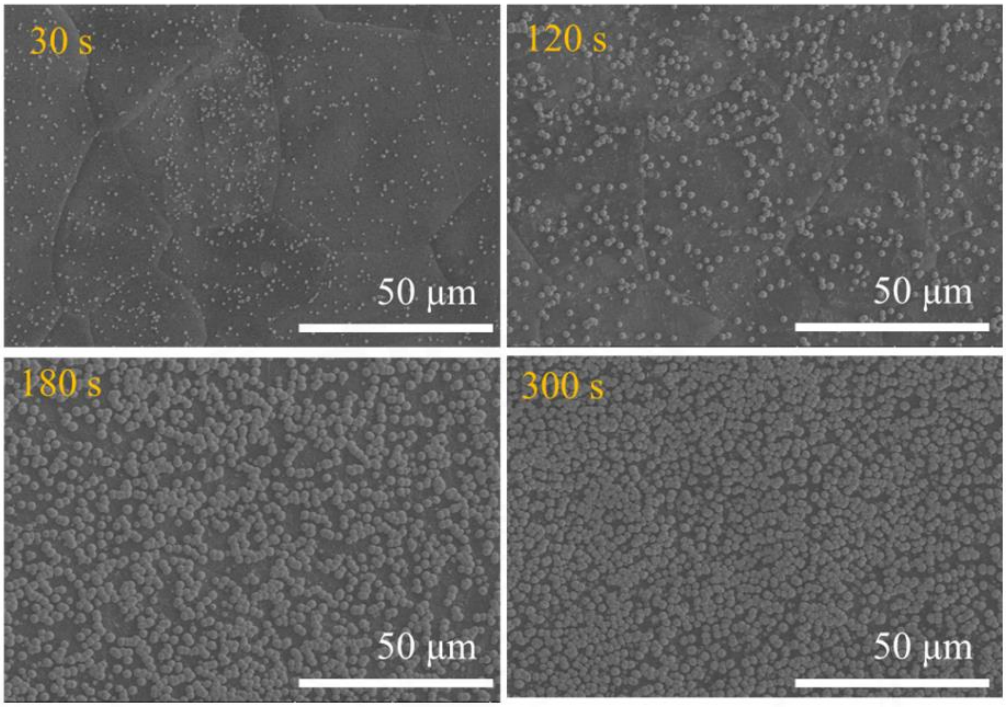

Figure 4.6 FE-SEM images of silver nanoparticle preparing by electrodeposition method at current density of 10 µA/cm^2 for 30 s, 120 s, 180 s, and 300 s.

The mechanical properties of the SERS substrate is important for practical field uses. Due to the limitation of preparing PDMS for this test, only the mechanical properties of the PI-SERS substrate were examined. The test investigated if the process of transferring the AgNPs/G/Cu onto PI followed by etching and baking deteriorates the mechanical property of the PI backing tape. The stress–strain plot of G/AgNPs/PI substrate compared to that of pristine PI tape is displayed in Figure 4.7. It was found that the elastic moduli from both samples were similar while the tensile strength and the elongation at break of the G/AgNPs/PI substrate was significantly higher than that of the pristine PI as shown in Table 4.2. This indicated that the process of transferring, etching, and annealing of the resulting SERS substrate did not deteriorate the property of the PI tape and in fact slightly enhanced it probably due to the property of the graphene layer, or the thermal annealing of the PI substrate after the transfering process.

Ref. code: 25655922300099OUH

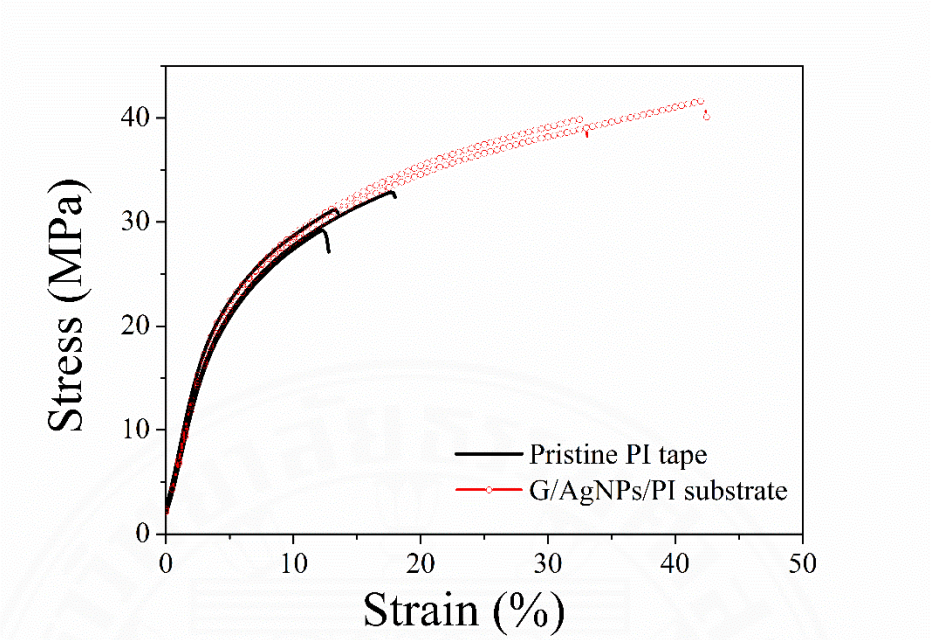

Figure 4.7 The stress–strain plot of G/AgNPs/PI substrate compared to that of pristine PI SERS substrate.

Table 4.2 Comparison of the mechanical properties of bare PI and PI SERS substrate

Sample	Tensile strength (Mpa)	Elastic modulus (Gpa)	Elongation at break (%)
PI	33.5 + 1.6	0.55 + 0.02	14.8 + 2.4
PI-SERS	36.7 + 5.7	0.54 + 0.03	28.7 + 13.3

4.3 Effect of excitation light source to Raman measurement

In Raman measurement, the excitation source must provide a high Raman signal for the analyte and low signal appearance from the substrate. The absorbance of PDMS and PI in the range of 400-800 nm were investigated in order to choose the proper laser source for Raman measurement. The absorbance of PDMS and PI substrate displayed in Figure 4.8 shows that PDMS does not absorb the spectra in the range 400-800 nm. While the PI absorbs light from 400-550 nm. Thus, the laser light source for PDMS should be in the range of 400-800 nm while the laser source for PI should be one larger than 550 nm. Thus, in this work the lasers source for PI is at 785 nm and PDMS can be

Ref. code: 25655922300099OUH

both 532 nm and 785 nm. The Raman spectra of PDMS SERS substrate with the excitation wavelength of 532 and 785 nm was compared and shown in Figure 4.9. It showed that with the 785 nm excitation laser source, the huge peak at 1300 cm^{-1} hinders the methyl parathion signal. This peak is the D peak of graphene which indicates defects of graphene that could be formed due to the high energy of 785 nm laser destroying the graphene layer. Therefore, the laser source chosen for the PDMS SERS substrate in this work is 532 nm

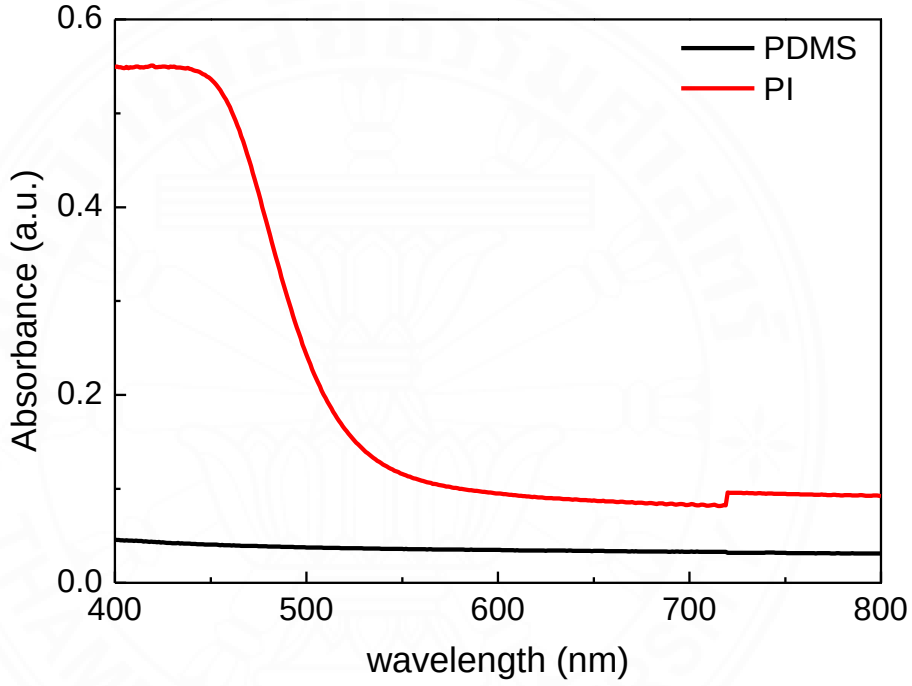

Figure 4.8 Absorbance of PDMS and PI substrate

Ref. code: 25655922300099OUH

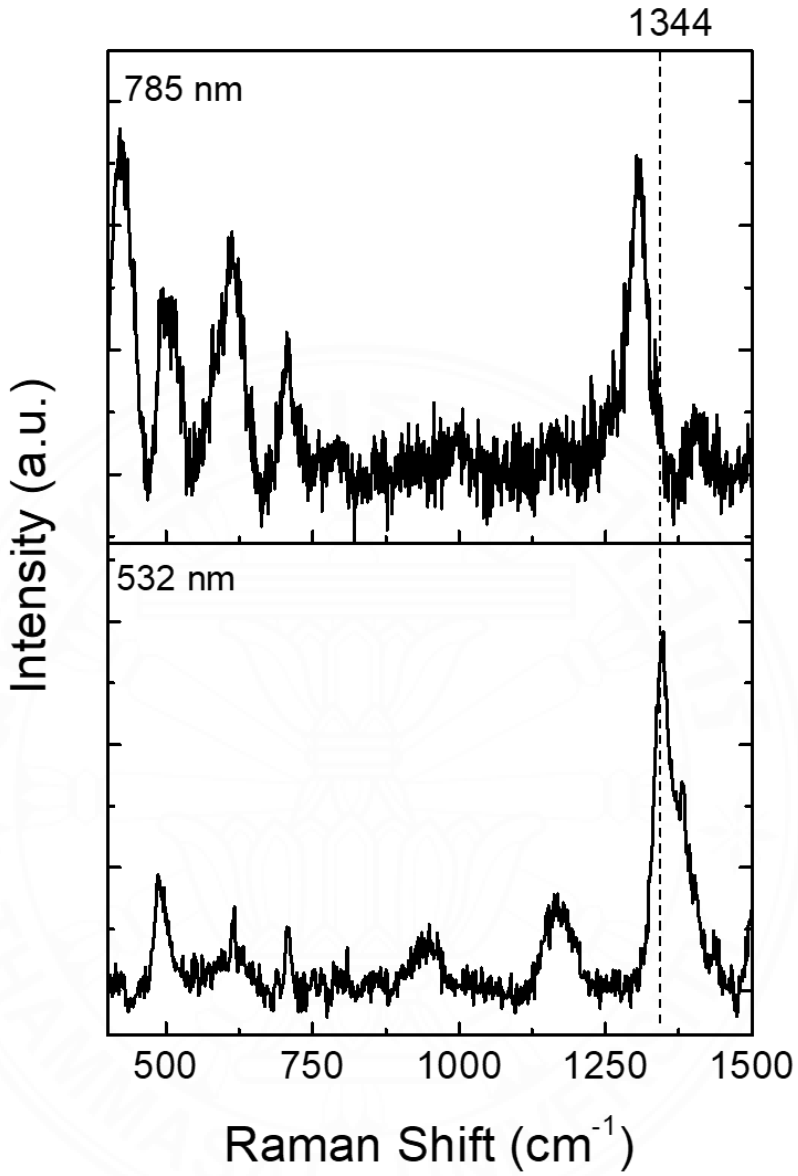

Figure 4.9 Raman spectra of methyl parathion on G/Ag/PDMS obtaining from 785 nm (top) and 532 nm (bottom) excitation laser source.

The Raman spectra of methyl parathion powder, PI and PDMS substrate, methyl parathion on substrate and methyl parathion on PDMS and PI SERS substrate are shown in Figure 4.10 and 4.11, respectively. The Raman spectra of methyl parathion powder show the primary vibration at 860, 1107, 1214, 1344 and 1591 cm^{-1} corresponding P-O, C-N, C-O, NO_2 and benzene ring, respectively. While the Raman signal of methyl parathion on G/Ag/PDMS SERS substrate shows the primary vibrations of MP at 860,

Ref. code: 25655922300099OUH

1135, 1344, and 1590 cm^{-1} corresponding to P-O, CC-H, NO_2 and benzene ring, respectively. However, Raman spectra at 1135 cm^{-1} are very low and the signal at 860 cm^{-1} and 1586 cm^{-1} is interfered by the PDMS and graphene. Therefore, only the peak at around 1344 cm^{-1} was used for analysis in this work. Similarly, the Raman signal of methyl parathion on G/Ag/PI shows interference of signal at the wave number 860 and 1108 by the PI substrate, and the signal at 1135 is quite low. Thus, only the peak at around 1344 cm^{-1} was used for analysis.

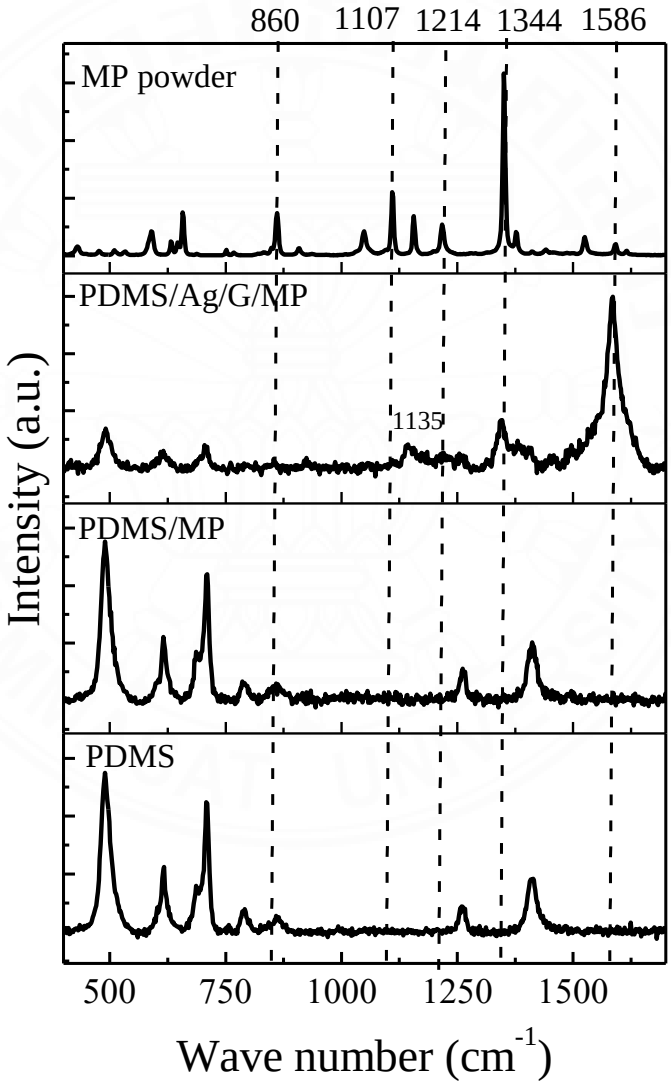

Figure 4.10 Raman spectra of PDMS substrate, methyl parathion on PDMS substrate, methyl parathion on G/Ag/PDMS SERS substrate and methyl parathion powder obtained by the 532 nm excitation source.

Ref. code: 25655922300099OUH

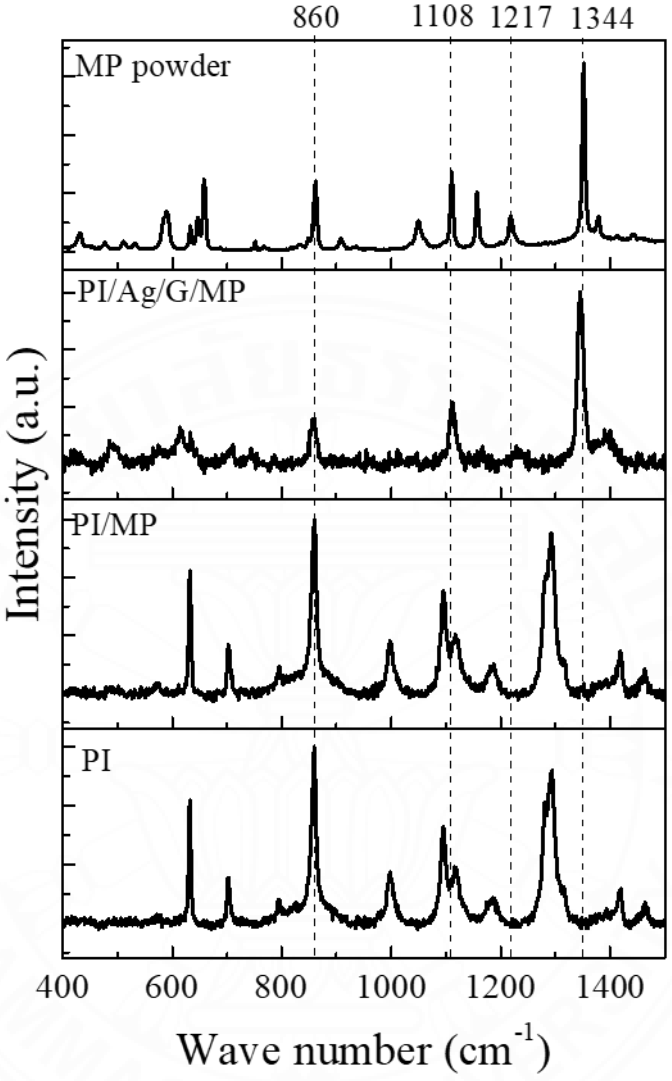

Figure 4.11 Raman spectra of the PI substrate, methyl parathion on PI substrate, methyl parathion on G/Ag/PI SERS substrate and methyl parathion powder obtained by the 785 nm excitation source.

4.4 Effect of current density, and deposition time to SERS performance

In order to investigate SERS performance, the SERS substrate was cut to 2 x 2 cm^2 and 4 µl of Methyl parathion was dropped on the SERS substrate for investigating the optimized condition of silver deposition for the best enhancement in Raman signal. Raman signal form ten random positions on the SERS substrate was collected and the average intensity at 1344 cm^{-1} was compared. The intensity of Raman signal from the

Ref. code: 25655922300099OUH

SERS substrate at different electrodeposition current densities and deposition times are shown in Figure 4.12.

To investigate the effect of current density, the various current densities at 1, 5, 10, 20, 50, 100 μAcm^{-2} were applied for 3 min. The results show that the SERS substrate prepared with current density at 10 μAcm^{-2} possesses the highest Raman intensity. Then silver nanoparticles were prepared at a fix current density of 10 μAcm^{-2}, and the deposition time was varied at 2, 3, 4, 5 minutes.

We found that the SERS substrate prepared with silver deposition at the current density of 10 μAcm^{-2} for 3 minutes yielded the best Raman signal. This condition is then selected and used for preparing subsequent SERS substrates for further investigation. These results could be explained by comparing them with the SEM results. Silver particles prepared by this condition provided gaps between particles in the range 50-100 nm and a gap between strands 30-100 nm which are a suitable size to function as a hot spot for SERS enhancement. Because the gaps between strands of the rattan ball like structure does not change with the current density, it provides a hot spot for all conditions. However, the different gap sizes between particles affect the number of hot spots for SERS. Thus, preparing silver nanoparticle at the current density 10 μAcm^{-2} for 3 minutes provides a good number of hot spots.

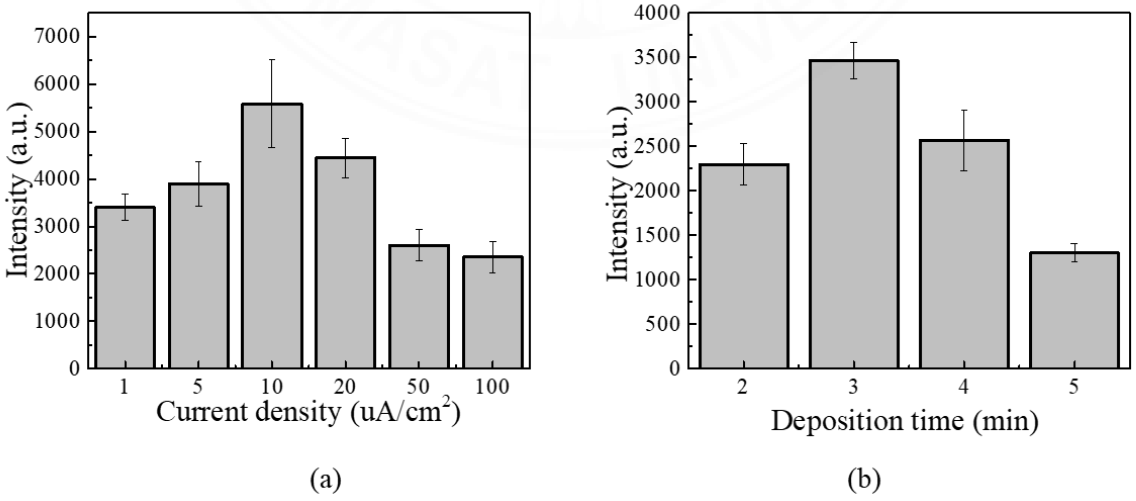

Figure 4.12 Intensity of Raman signal from SERS substrate at different electrodeposition current densities (a) and deposition times (b)

Ref. code: 25655922300099OUH

4.5 Effect of graphene and the enhancement mechanisms

The enhancement for Raman signal could be by two mechanisms: electromagnetic and chemical enhancement. In this work, the Raman enhancement was mainly generated from the electromagnetic enhancement which is due to methyl parathion molecules being adsorbed onto the hot spots of silver nanoparticles on the SERS substrate. Without the silver nanoparticles, the bare MP signal was barely observed. As shown in Figure 4.10 and 4.11, the Raman enhancement of MP appear in the G/Ag/PDMS and G/Ag/PI substrates. In both substrates, four dominant vibration modes of MP molecules that were strongly enhanced were at frequencies 860, 1135, 1344 and 1590 cm^{-1} corresponding to the P-O, CC-N, N-O and the phenyl stretching vibrations, respectively. In addition, Figure 4.13 shows the effect of the graphene coverage on the silver nanoparticles, which could enhance the Raman signal slightly further. The graphene layer probably promoted the chemical enhancement by improving the charge transfer between the MP and the silver nanoparticles, and thus enhancing the electromagnetic enhancement slightly further.

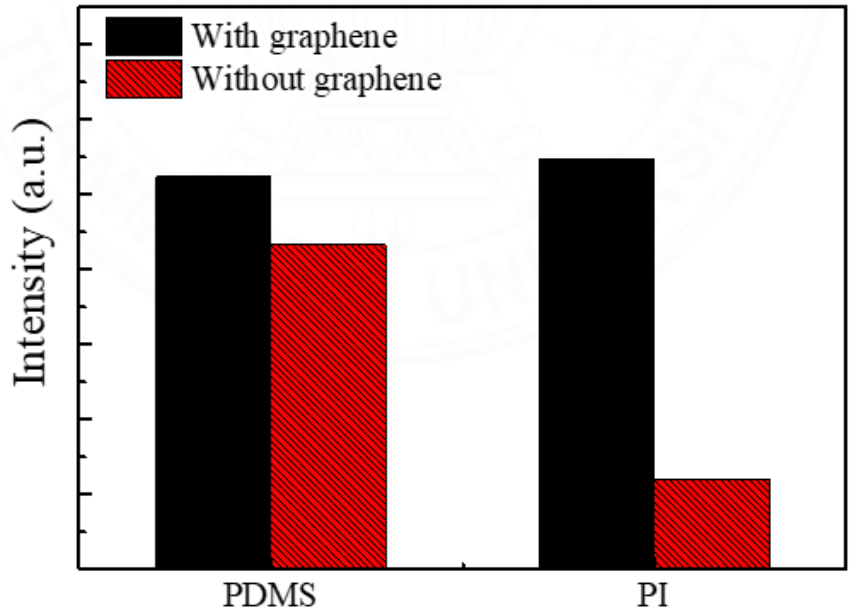

Figure 4.13 The intensity of the Raman signal at wave number 1344 cm^{-1} obtained by PDMS and PI SERS substrate with and without graphene coverage.

Ref. code: 25655922300099OUH

4.6 Sensitivity of SERS substrate

In order to determine the sensitivity of the SERS sensor, methyl parathion (MP) in ethanol was prepared at the concentration range from $2.5x10^{-5}$ M to $1x10^{-3}$ M. The SERs substrate was cut into a dimension of 2x3 mm^2, four microliters of methyl parathion solution were dropped onto the SERS substrate and allowed to air dry for 30 min before performing Raman measurement. The primary peak at 1344 cm^{-1} was used for examining the Raman signal. The data was pre-processed by normalizing with the spectral mean and using extended multiplicative scatter (EMSC) correction.

The relationship between Raman signal intensity and methyl parathion concentration was investigated. The results in Figure 4.14 show a linear response of the Raman signal to the methyl parathion concentration with $R^2 = 0.84$ and 0.93 for PDMS and PI SERS substrate, respectively. The limit of detection (LOD) of methyl parathion estimated by 3.3SD/slope is about $8x10^{-4}$ and $5x10^{-4}$ M for PDMS and PI SERS substrate, respectively. The enhancement factor was estimated from equation 1 by using the SERS signal and comparing it with the Raman signal. Due to the low Raman signal from MP on bare PI substrate, only the high concentration at 10^{-2} M of methyl parathion can be measured. Thus, the calculated enhancement factor was obtained from the signal of $1x10^{-3}$ M methyl parathion on SERS substrate compared to the Raman signal of 10^{-2} M methyl parathion on a bare substrate. The calculated enhancement factor for PDMS SERS substrate is $1.48 x10^4$ while it is about $4.7 x 10^4$ for PI SERS substrate.

Ref. code: 25655922300099OUH

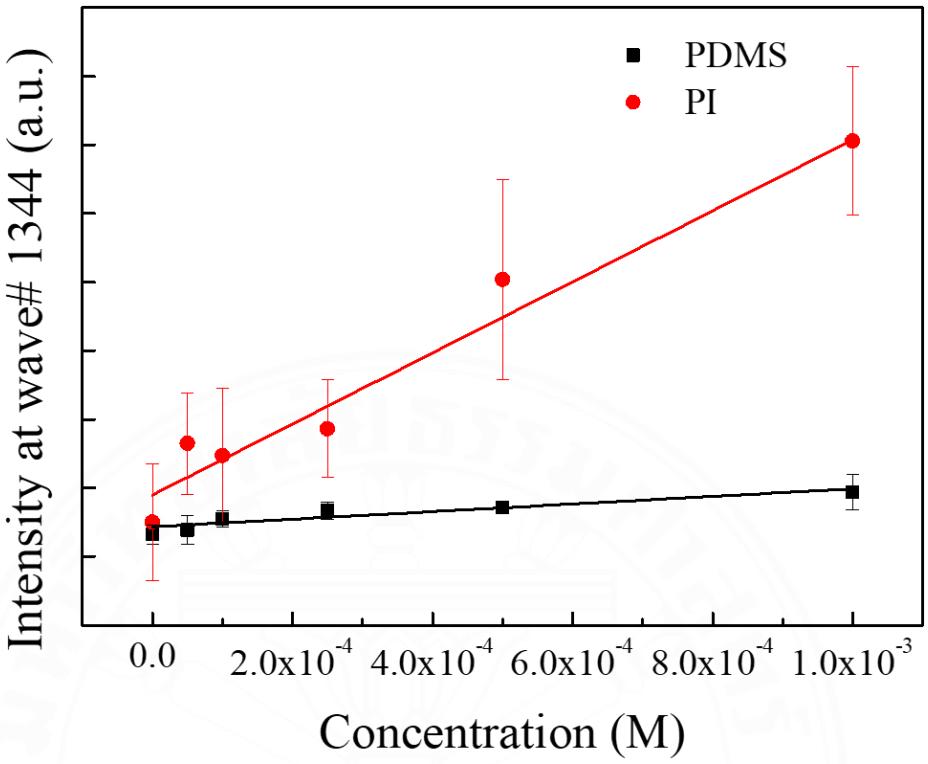

Figure 4.14 Linear relationship between methyl parathion concentration and the normalized intensity of the Raman signal at wave number 1344 cm^{-1}

4.7 Uniformity of SERS substrate

The uniformity of the SERS substrate was examined by measuring the Raman spectra at several random positions on the SERS substrate. The SERS substrate was cut into 2 x 2 cm^2 sheets, the 1 mM methyl parathion was dropped in the center and at the 4 corners of the SERS substrate, and then Raman signals from 20 spots on the sensor were collected. The data was preprocessed by normalized with spectral mean after correction with the extended multiplicative scatter (EMSC) correction (Liland et al., 2016). The Raman spectra together with the intensity of the peak at the wave number 1344 cm^{-1} from each spot on the PMDS (PI) SERS substrate are shown in Figure 4.15 (Figure 4.16).

The results demonstrate the similar Raman profile without the significant shift of the signals. The intensity at 1344 cm^{-1} from these spots were also compared and the relative standard deviation (RSD) was calculated to be about 25% and 11% for the

Ref. code: 25655922300099OUH

PDMS and PI substrate, respectively. Compared with the other research group that report the RSD in the range of 5-20% (Liu et al., 2014; Sun et al., 2017; Wang et al., 2014; Yu et al., 2018), %RSD of our PDMS SERS substrate is quite high, while the obtained RSD for PI is acceptable. The non-uniformity in the substrate might be from the silver electrodeposition process as well as the transferring process. During the silver decoration process, electrodeposition was done in a stirred electrolyte. The micro-stream of electrolytes might cause a non-uniform distribution of silver particles in each area of the substrate. While in the transferring process, the curing of the PDMS might cause some non-uniformity which creates the non-uniform structure on PDMS SERS substrate.

Ref. code: 25655922300099OUH

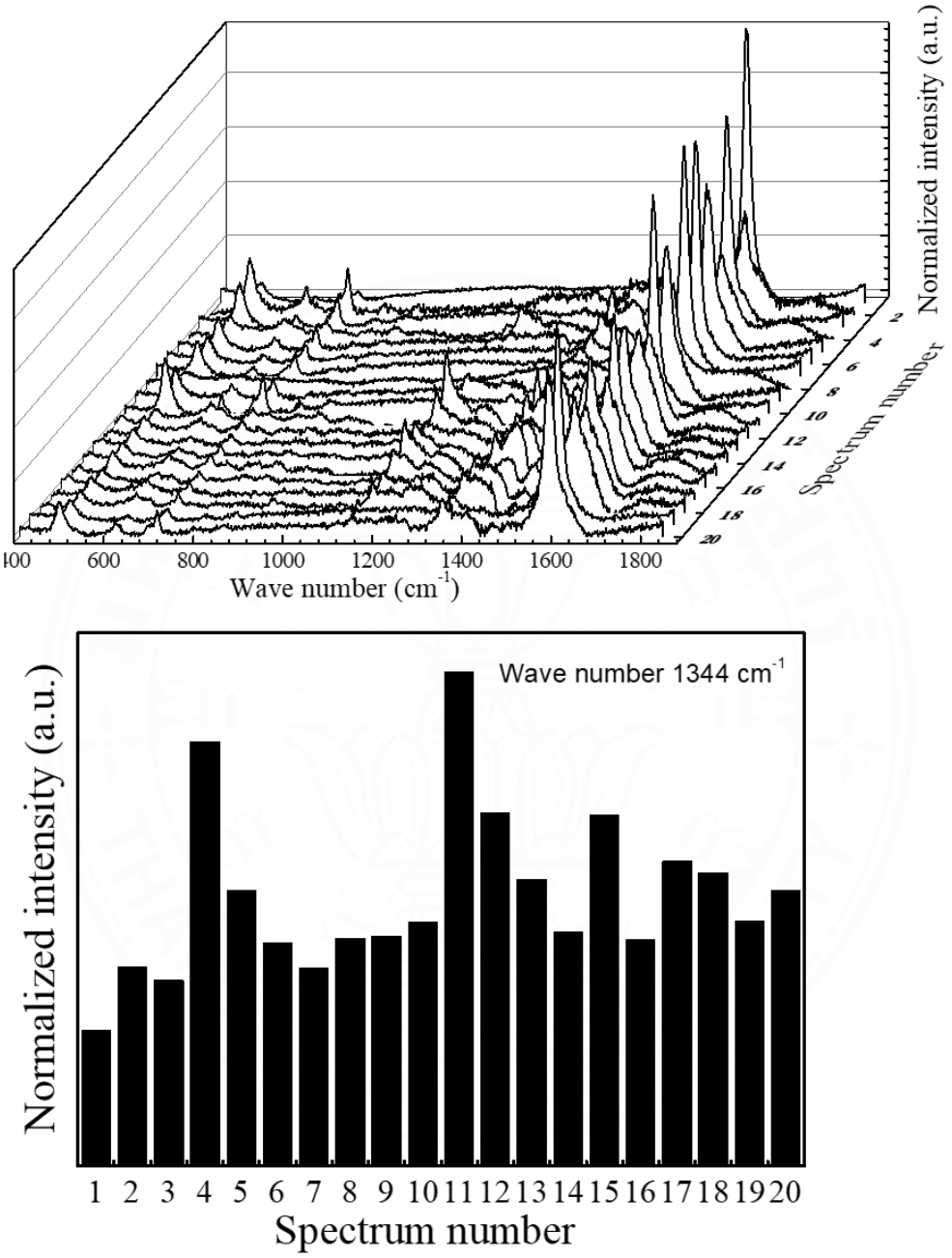

Figure 4.15 Plot of Raman spectra (top) and Raman intensity at 1,344 cm^{-1} (bottom) of each spot for the PMDS SERS substrate. At 1,344 cm^{-1}, the %RSD relative to the mean intensity was calculated to be 25%.

Ref. code: 25655922300099OUH

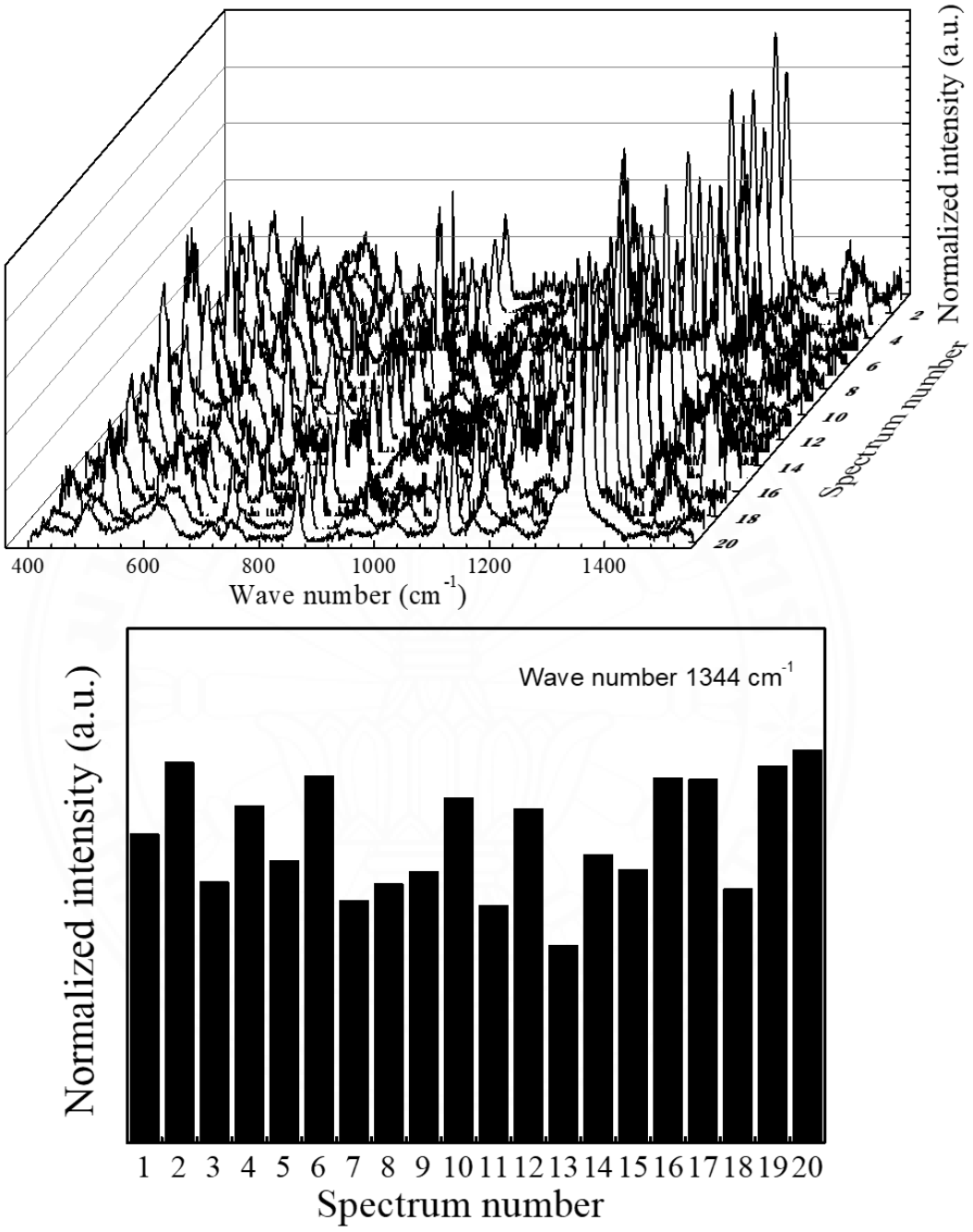

Figure 4.16 Plot of Raman spectra (top) and Raman intensity at 1,344 cm^{-1} (bottom) of each spot for the PI SERS substrate. At 1,344 cm^{-1}, the %RSD relative to the mean intensity was calculated to be 11%.

Ref. code: 25655922300099OUH

4.8 Stability of SERS substrate

The stability of our SERS substrate was investigated by comparing the SERS signal from the sensor with and without graphene coverage as a function of storage times. SERS substrates were prepared and kept in two conditions: the normal atmosphere and room temperature of about 27-32 ℃ (RT/ambient air) and in the desiccator with controlled temperature and relative humidity (RH) at 25 ºC and 40%RH, respectively. The 2x2 cm^2 SERS substrate was prepared and cut into 2x3 mm^2 sheets for each Raman measurement. An average of 5 SERS signals at 1,344 cm^{-1} were collected over time.

The results in Figure 4.17 show the relationship of storage time and relative intensity of Raman signal I/I_0, while I and I_0 are the intensity of the PDMS SERS substrate at the measured date and at the freshly prepared date, respectively.

A similar trend was found in a SERS substrate kept in normal room temperature and in a desiccator that the intensity decreases over time, but the decreasing rate of intensity is faster in case of SERS stored in ambient air.

After 48 days, the Raman intensity percentage of PDMS SERS substrate left in ambient air condition without graphene protected layer decreases sharply to the value of only 3.6%. While samples with graphene protected layer was still working with the intensity percentage of 57.6%. PDMS SERS substrates kept in a desiccator show better results, the intensity percentage of the SERS substrate is at about 87.1% and 36.8% for substrate with and without a graphene layer.

The relationship of storage time and the relative intensity of Raman signal I/I_0 of PI SERS substates are shown in Figure 4.18. The top figure is the result of the SERS substate stored at ambient air for 48 days, it was found that SERS substrates without a graphene protected layer were not in working condition while the ones with a graphene protected layer still showed a Raman signal with the intensity percentage of 12.6% compared to the freshly prepared sample. SERS substrates stored in a desiccator show that after 48 days the Raman signal measured from SERS substrate with and without a graphene protected layer was 42.1% and 22.8%, respectively.

Ref. code: 25655922300099OUH

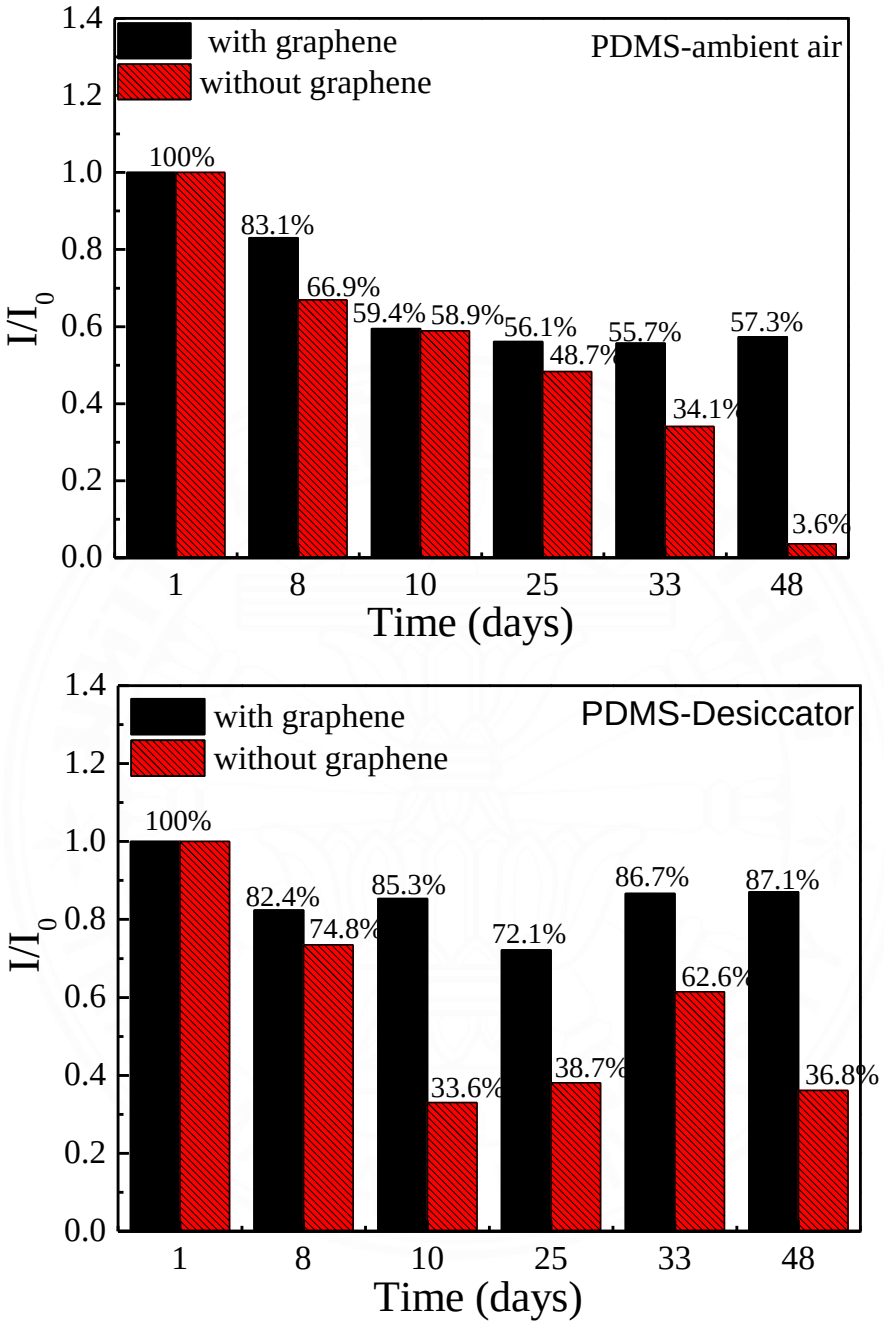

Figure 4.17 The Raman intensity at wave number 1344 cm^{-1} of the PDMS SERS substrate as a function of storage time under ambient air (top) and under a desiccator at 25 °C and 40%RH (bottom).

Ref. code: 25655922300099OUH

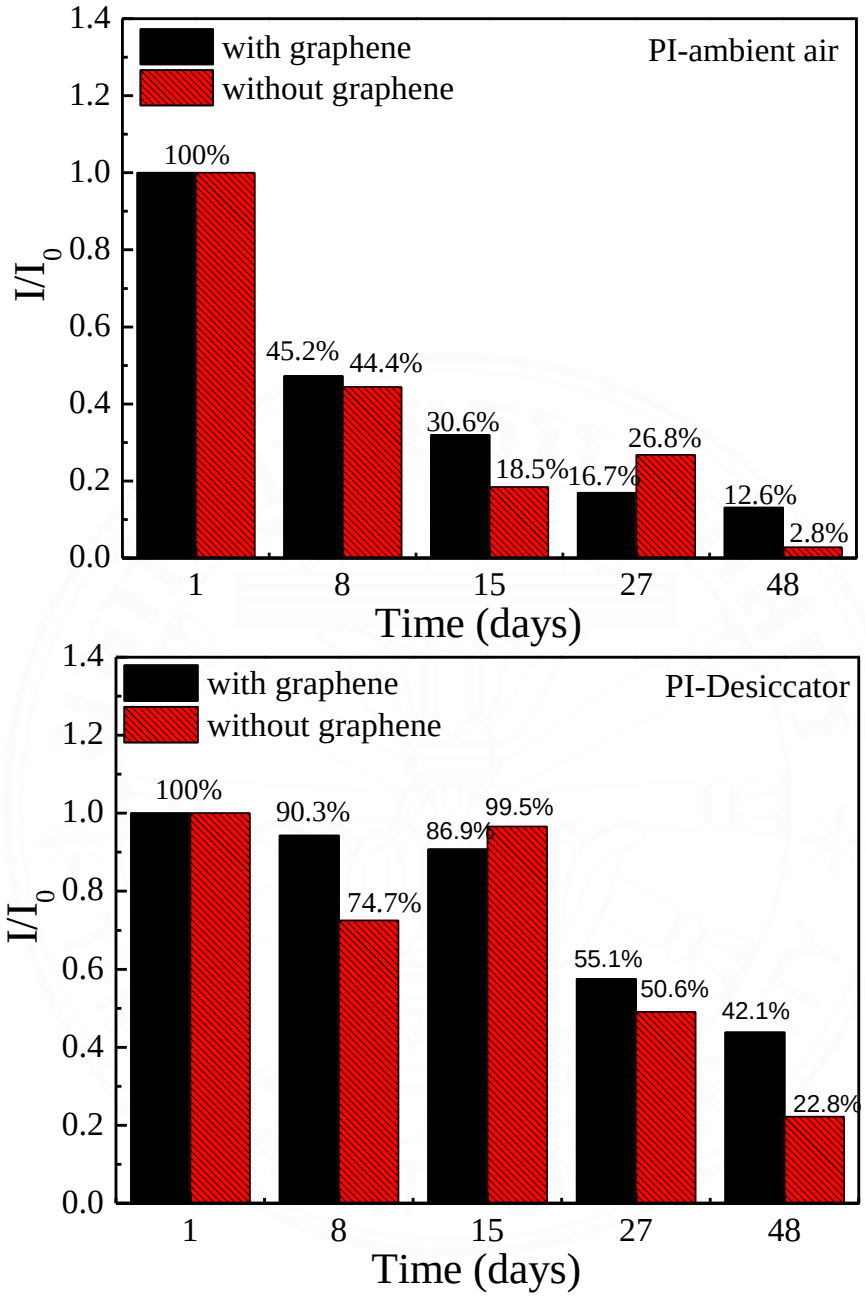

Figure 4.18 The Raman intensity at wave number 1344 cm^{-1} of the PI SERS substrate as a function of storage time under ambient air (top) and under a desiccator at 25 °C and 40%RH (bottom)

This can be explained in terms of the decent coverage of graphene on top of silver nanoparticles isolating the silver from the ambient oxygen and other potentially contaminating gases in the environment. It indicates that that graphene is efficiently

Ref. code: 25655922300099OUH

protecting the silver from getting oxidized. Moreover, from observation, the intensity of the substrate with graphene is higher than that of one without graphene. Therefore, graphene plays a role in enhancing the Raman signal and as a protection layer for the SERS substrate. Thus, graphene helps extend the shelf life for SERS substrate and keeps it in proper condition.

4.9 Testing SERS substrate with real sample

The SERS substrate was tested in real conditions by dropping a 1mM methyl parathion (MP) on an apple, waiting until it dried, then attaching the SERS pad on top of that area and finally measuring from the back side of sensor. The Raman signal of an apple, the apple/SERS, the MP coated on the apple, and the MP/SERS substrate on the apple were collected. Figure 4.19 and Figure 4.20 show the Raman signal of MP on the apple using the PDMS and PI SERS substrate, respectively. It can be seen that without the use of SERS, MP Raman signal on the apple could not be detected, while the MP Raman signal can be easily detected with the use of SERS substrate both PI and PDMS.

Ref. code: 25655922300099OUH

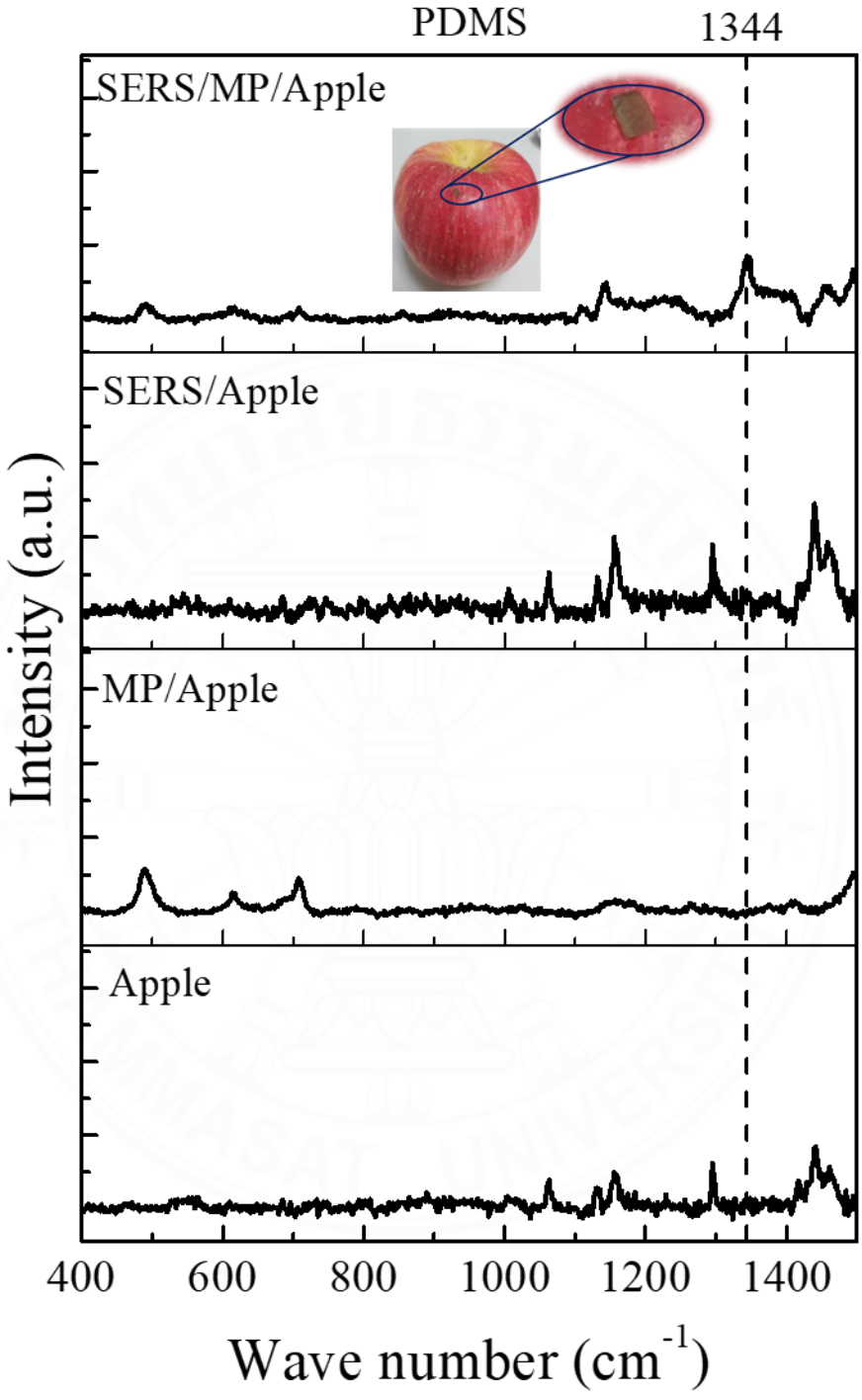

Figure 4.19 Raman spectra of methyl parathion residue on apple detected by PDMS SERS substrate.

Ref. code: 25655922300099OUH

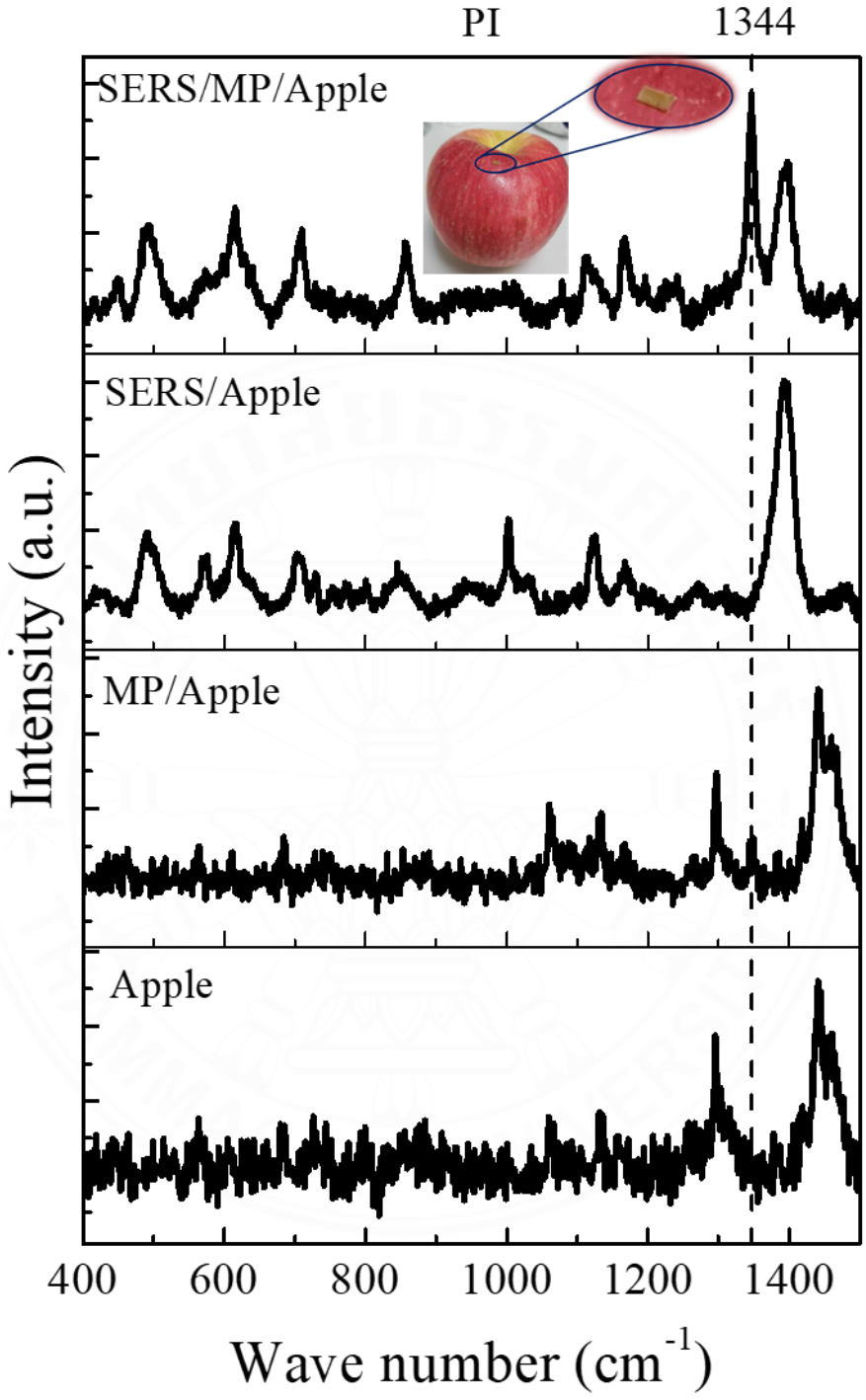

Figure 4.20 Raman spectra of methyl parathion residue on apple detected by PI SERS substrate.

Ref. code: 25655922300099OUH

The detection limit for detecting MP on a real sample of apple fruit was investigated by preparing methyl parathion (MP) in ethanol at the concentration range from 5-75 M. The primary peak at 1344 cm^{-1} was used for examining the Raman signal. The data was pre-processed by normalizing with the spectral mean and using extended multiplicative scatter (EMSC) correction. The relationship between Raman signal intensity and methyl parathion concentration was investigated. The results in Figure 4.21 show a linear response of the Raman signal to the methyl parathion concentration with R^2 = 0.91 and 0.98 for PDMS and PI SERS substrate, respectively. The limit of detection (LOD) of methyl parathion, estimated by 3.3SD/slope is about 35 mM and 16 mM for PDMS and PI SERS substrate, respectively.

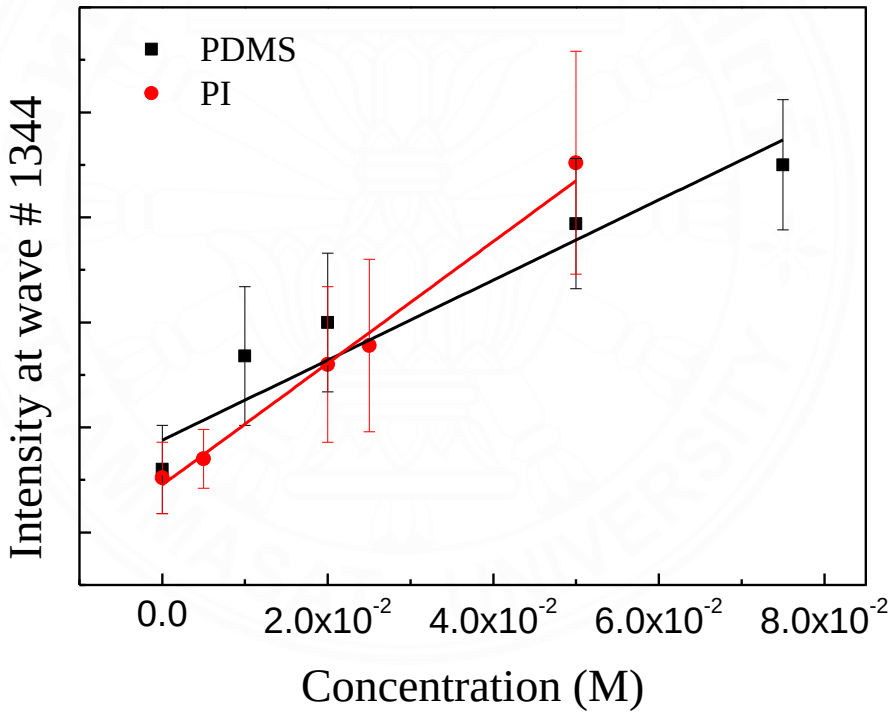

Figure 4.21 Linear relationship between methyl parathion concentration and the normalized intensity of the Raman signal at wave number 1344 cm^{-1} of Raman signal on apple

The recovery tests were performed by measuring the three levels of spike methyl parathion (20, 25 and 50 mM) on apple compared with the known concentration as shown in the table 4.3. The recovery is in the range 91-142% and 82-98% for PDMS

Ref. code: 25655922300099OUH

and PI SERS substrate, respectively. The results confirm that our SERS substrate could be used for methyl parathion residue detection for real sample.

Table 4.3 Recovery test of methyl parathion on apple

Spiked concentration (mM)	PDMS		PI	
	Detected concentration (mM)	Recovery (%) (n=20)	Detected concentration (mM)	Recovery (%) (n=20)
20	18.3	91.7	19.6	98
25	35.4	142	22.5	90.3
50	59.9	120.0	41.1	82.3

The LOD of these polymer substrates for detection of residue pesticide on real sample is not superior due to the measurement on the back side of the polymer lead to the difficulty to focus the laser light. However, this result demonstrates the high potential of the developed SERS for its flexible applications in field usage.

4.10 Suggestions for Future Research

4.10.1 Additional polymer-based SERS

Alternative materials could be used for fabricating a flexible SERS substrate by the techniques propose in this report. We prepared a SERS substrate using other types of commercial tape and natural rubber. Figure 4.22 shows the Raman signal of 1 mM Methyl parathion measuring by SERS substrate with commercial tape including clear tape, net tape, and very high bond tape (VHB tape). It was found that those commercial tapes can be used as a SERS substrate. However, preparing a natural rubber-based SERS was not successful because it could not withstand the etching chemical. Therefore, the fabrication technique propose in this thesis could be applied to another type of polymer if it is transparent, does not absorbed the excitation laser and the Raman peak does not coincide with the tested sample. The promising material could be Teflon, PE tape, or PVDA etc.

Ref. code: 25655922300099OUH

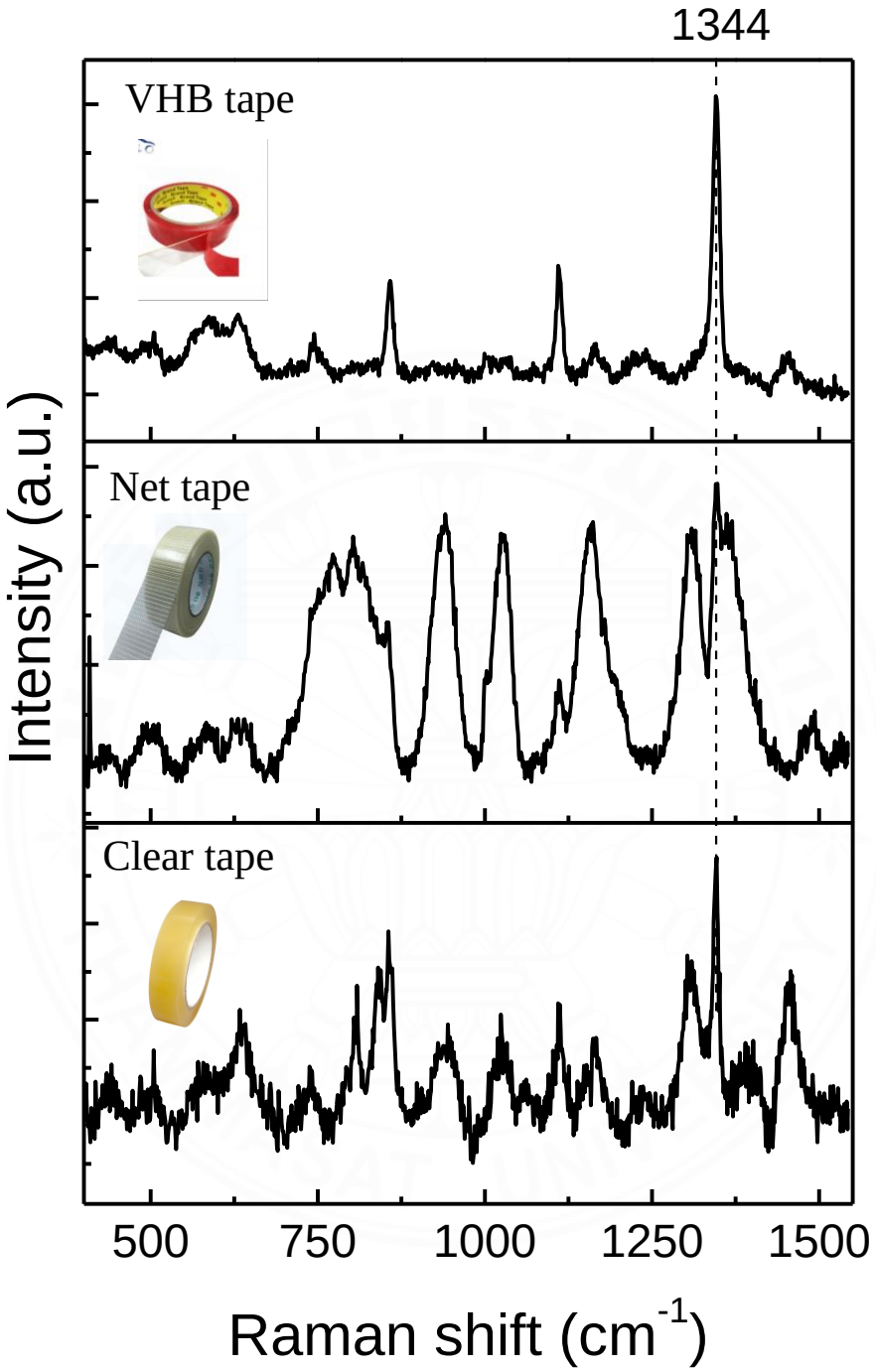

Figure 4.22 Raman signal of 1 mM methyl parathion measuring by SERS substrate preparing with clear tape, net tape, and very high bond tape (VHB tape)

Ref. code: 25655922300099OUH

4.10.2 Preparation of Ag nanoparticle by sputtering technique

Sputtering is commonly used for thin film preparation. The metal target was knocked by a plasma of inert gas to allow the material ions to coat the substrate. In this work, we used sputtering to prepare the SERS substrate to see if it shows similar results with the electrodeposition technique. Ag nanoparticles were coated on a graphene/Cu by DC sputtering at 0.2 A under argon gas. The SEM image in Figure 4.23 (a) shows the graphene wrinkle with small silver particles on top. The silver particles evenly covered over the graphene surface and as the sputtering time increased, the particle sizes were larger and covered all the area before it started to grow on the top layer of the as prepared and made it thicker. As the sputtering time increased, the Ag film thickened. While preparing a SERS substrate by transferring the Ag/graphene/Cu on the PDMS and measured Raman signal of methyl parathion, we found that the SERS substrate prepared by sputtering Ag for 15 s showed the best result (Figure 4.23 (b). This is consistent with the SEM results that show that there are some gaps between the Ag nanoparticles. However, the sensitivity of this SERS substrate for methyl parathion detection is still not high, which could be the result of oxidation of the silver film after the $FeCl_3$ etching process.

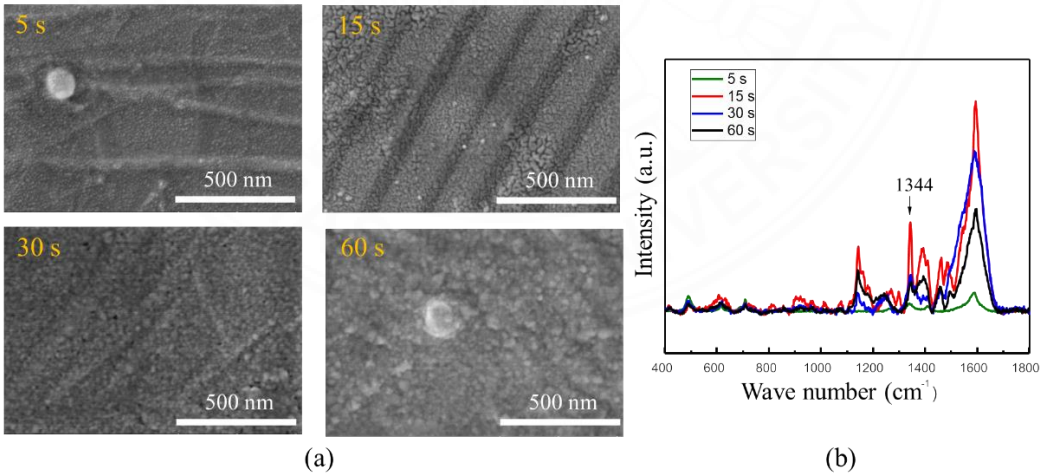

Figure 4.23 FE-SEM images of silver nanoparticle preparing by sputtering method at an applied current of 0.2 A for 5 s, 15 s, 30 s, and 60 s (a) and the Raman signal of methyl parathion on the SERS substrate preparing by various sputtering time.

Ref. code: 25655922300099OUH

4.10.3 AgO elimination

As shown in the previous section, the oxidation of the Ag nanoparticles (AgO) was the result of the etching process. Thus, the AgO elimination may be able to enhance the SERS performance further. Hydrogen plasma is well-known as a strong reducing agent and could be used to remove oxide from the metal surface. In this work, hydrogen plasma treatment was tested for removal of the oxidation on the SERS substrate. Hydrogen plasma was generated by an inductively coupled plasma (ICP) with a power of 100 Watt for 10 min. The SEM images of the SERS substrate before and after hydrogen treatment is shown in Fig 4.24. Treating with hydrogen plasma polished the Ag nanoparticles, so the sharp edges were gone. Those lowered the hot spot number of the SERS substrate which caused a lower Raman enhancement. Therefore, to improve the SERS substrate fabricated by this technique, another method for removing AgO should be further studied. One possibility could be to use a non-oxidized Cu etchant solution such as a HCl, ammonium persulfate or using a chemical reduction process after Cu etching.

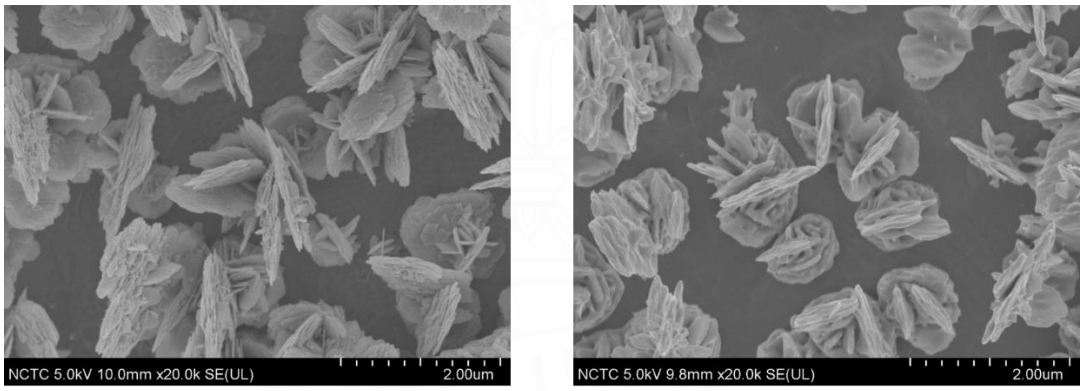

(a) (b)

Figure 4.24 FE-SEM images of silver nanoparticle on graphene/Cu substrate (a), and after hydrogen treatment (b)

4.11 Summary

A flexible SERS substrate based on graphene/Ag/polymer composite layered structure was successfully fabricated with the polymer layer being either the PDMS or the polyimide (PI) tape. The developed SERS substrate could detect methyl parathion

Ref. code: 25655922300099OUH

with the enhancement factors (EF) at the methyl parathion primary peak (1,344 cm^{-1}) of $1.5x10^4$ and $4.x10^4$ for the PMDS and PI SERS substrate, respectively. The SERS substrate was also used for detecting MP on a real sample of apple fruit and it could detect the MP in the mM range concentration. The shelf life of the G/Ag/PI substrate, kept at room temperature, was extended to be longer than 48 days. Compare between two types of substrates, we found that PDMS is better in the enhancement factor and extended shelf life. However, the uniformity of prepared PI SERS substrate is better than PDMS SERS substrate. The recovery test was performed to verify the reliability of the method, and it was found that the recovery is in the range 91-142% and 82-98% for PDMS and PI SERS substrate, respectively. The sensitivity of both SERS substrates is moderate which is the result of oxidation occurring after the etching process. To overcome these problems, hydrogen plasma was used and did not provide a good result probably because the plasma smoothen out the hot spots of SERS substrate. Therefore, another option such as Cu etchant and the chemical reduction process could be applied to increase SERS performance. Although, the LOD of these polymer substrates did not provide a superior enhancement performance, it did offer facile fabrication, low cost, and longer shelf life. This polymer-based SERS substrate offers a promising hybrid platform with the potential to be significantly used as a screening technique in field tests. Moreover, other types of polymers could also be applied along with this technique to improve this polymer-based SERS sensor.

Ref. code: 25655922300099OUH

CHAPTER 5
CONCLUSIONS

Raman spectroscopy is a rapid chemical analysis technique which can be used as a powerful tool to detect molecules via their Raman spectral fingerprint. However, the limitation of this technique for an identified material is that the Raman signal is typically weak and thus difficult to collect the signal. Surface-enhanced Raman spectroscopy or surface-enhanced Raman scattering is a surface sensitive technique that enhances the Raman signal by using adsorption of molecules on a rough metal surface. In this work, a flexible film-based SERS that consists of polymer as a substrate and protective layer, silver nanoparticles as a metal for Raman enhancement, and graphene as a conductive protective layer (G/Ag/polymer) were fabricated.

The graphene functions as a protective layer of the SERS substrate and assists also in the enhancement of Raman signal. It was prepared by chemical vapor deposition (CVD) technique on a copper foil. With this technique, a few layers graphene could be obtained which was confirmed by the intensity ratio of the 2D to the G band (I_{2D}/I_G) in the Raman spectra. Silver nanoparticle as an enhancement material was coated on graphene by the electrodeposition technique. Silver nitrate with citric acid solution was used as a silver source with the citrate ions play roles of reducing agent a controlling shape. The structure of the silver nanoparticle growth on graphene/copper can be tuned by varying the electrodeposition conditions. The best Raman enhancement signal was obtained by electrodeposition at the current density of 10 μA cm^{-2} for 3 min. This condition provides rattan ball-like silver nanoparticles with hierarchical gaps in the silver rattan-ball structures varying between 30-100 nm and seems to best enhance Raman signal.

The as-prepared layers were then transferred onto the polymer layer which functions as a supporting material and also as the silver protective layer. Two types of polymers were used in this work: PDMS and polyimide tape. PDMS was prepared by spin coating technique to obtain a PDMS thickness of about 150 μm, robust enough for easy handling, and thin enough for the laser light to pass though. For the polyimide tape (PI), the tape was mechanically pressed on top of the prepared silver then it was heated

Ref. code: 25655922300099OUH

at 80 ^{o}C for 15 min. After applying the polymer on top of the prepared substrate, copper foil was removed by chemical etching using a ferric chloride solution ($FeCl_3$). The ferric chloride concentration and etching time was also optimized. A high concentration of ferric chloride allows fast etching but might destroy the transfer pattern. A slow etching is not good for mass production. In this work, copper was etched by a 40 mg/ml of ferric chloride for 1.5 and 2 h for PDMS and PI substrate.

The developed SERS substrates could detect methyl parathion with the enhancement factor (EF) of the primary peak at 1344 cm^{-1} of $1.5x10^4$ and $4.7x10^4$ for the PMDS and PI SERS substrates, respectively. The shelf life of the G/Ag/polymer substrate, kept at room temperature, was extended to be longer than 48 days comparing with the SERS substrate without graphene layer. Moreover, keeping the SERS substrate in the desiccator will further extend the shelf life without an additional packaging process.

The uniformity of SERS substrate was considered by a relative standard deviation (RSD) of 20 Raman signals collected from a 2 x 2 cm^2 SERS substrate. The RSD is calculated to be about 25% and 11% for PDMS and PI substrate, respectively. RSD of our PDMS SERS substrate is quite high, while the obtained RSD for PI is acceptable. The non-uniform substrate might be from the silver decoration and transferring process. During the silver decoration process, electrodeposition was done in a stirred electrolyte. The micro-stream of electrolytes might cause a non-uniform distribution of silver particles in each area of the substrate. This problem could be solved by using a large container for electrolyte which could reduce this effect. In the transferring process, due to the curing of PDMS, it might cause an unevenness which creates the non-uniform structure on PDMS SERS substrate.

The detection of MP on a real sample of apple fruit was investigated by dropping methyl parathion (MP) in ethanol on the apple and measured Raman signal. The limit of detection (LOD) of methyl parathion, estimated by 3.3SD/slope is about 35 mM and 16 mM for PDMS and PI SERS substrate, respectively. The recovery tests were performed by measuring the three levels of spike methyl parathion (20, 25 and 50 mM) on apple compared with the known concentration. The results show that the

Ref. code: 25655922300099OUH

recovery is in the range 91-142% and 82-98% for PDMS and PI SERS substrate, respectively.

Comparing the two types of substrates, we found that PDMS is better in the enhancement factor and has a longer shelf life, although the PI SERS substrate has better uniformity than that of the PDMS SERS substrate. The graphene layer also helps significantly extend the storage life of the substrate compared to that with the graphene layer. The developed G/Ag/polymer SERS substrate offer facile fabrication, low cost, and a longer shelf life. This polymer-based SERS substrate offers a promising platform with the potential to be significantly used as a screening technique in field tests.

Elimination of the oxidation of the Ag nanoparticles (AgO) resulting from the etching process is still the crucial challenge for this type of SERS substrate, which can lead to an improvement of the Raman enhancement for this polymer SERS substrate. Additionally, preparing a controllable metal morphology by other techniques such as Anodic Aluminum Oxide (AAO) template, Glancing Angle Deposition (GLAD sputtering) and chemical process could provide superior Raman enhancement.

Ref. code: 25655922300099OUH

REFERENCES

Albrecht, M. G., & Creighton, J. A. (1977). Anomalously intense Raman spectra of pyridine at a silver electrode. *Journal of the American Chemical Society*, *99*(15), 5215-5217. https://doi.org/10.1021/ja00457a071

Ayhan, M. E. (2020). A single-step fabrication of Ag nanoparticles and CVD graphene hybrid nanostructure as SERS substrate. *Microelectronic Engineering*, *233*, 111421. https://doi.org/https://doi.org/10.1016/j.mee.2020.111421

Budner, B., Kuźma, M., Nasiłowska, B., Bartosewicz, B., Liszewska, M., & Jankiewicz, B. J. (2019). Fabrication of silver nanoisland films by pulsed laser deposition for surface-enhanced Raman spectroscopy. *Beilstein Journal of Nanotechnology*, *10*, 882-893.

Chen, Y.-T., Pan, L., Horneber, A., Berg, M. v. d., Miao, P., Xu, P., . . . Zhang, D. (2019). Charge transfer and electromagnetic enhancement processes revealed in the SERS and TERS of a CoPc thin film. *Nanophotonics*, *8*(9), 1533-1546. https://doi.org/doi:10.1515/nanoph-2019-0100

Choi, C. J., Xu, Z., Wu, H.-Y., Liu, G. L., & Cunningham, B. T. (2010). Surface-enhanced Raman nanodomes. *Nanotechnology*, *21*(41), 415301. https://doi.org/10.1088/0957-4484/21/41/415301

Chu, F., Yan, S., Zheng, J., Zhang, L., Zhang, H., Yu, K., . . . Huang, Y. (2018). A Simple Laser Ablation-Assisted Method for Fabrication of Superhydrophobic SERS Substrate on Teflon Film. *Nanoscale Research Letters*, *13*(1), 244. https://doi.org/10.1186/s11671-018-2658-3

Coluccio, M. L., Das, G., Mecarini, F., Gentile, F., Pujia, A., Bava, L., . . . Di Fabrizio, E. (2009). Silver-based surface enhanced Raman scattering (SERS) substrate fabrication using nanolithography and site selective electroless deposition. *Microelectronic Engineering*, *86*(4), 1085-1088. https://doi.org/https://doi.org/10.1016/j.mee.2008.12.061

Cozzens, R. F., & Fox, R. B. (1978). Infrared laser ablation of polymers. *Polymer Engineering & Science*, *18*(11), 900-904. https://doi.org/https://doi.org/10.1002/pen.760181113

Fioravanti, F., Muñetón Arboleda, D., Lacconi, G. I., & Ibañez, F. J. (2020). Characterization of SERS platforms designed by electrophoretic deposition on CVD graphene and ITO/glass. *Materials Advances*, *1*(6), 1716-1725. https://doi.org/10.1039/D0MA00333F

Firet, N. J., Blommaert, M. A., Burdyny, T., Venugopal, A., Bohra, D., Longo, A., & Smith, W. A. (2019). Operando EXAFS study reveals presence of oxygen in oxide-derived silver catalysts for electrochemical CO2 reduction. *Journal of Materials Chemistry A*, *7*(6), 2597-2607. https://doi.org/10.1039/C8TA10412C

Fleischmann, M., Hendra, P. J., & McQuillan, A. J. (1974). Raman spectra of pyridine adsorbed at a silver electrode. *Chemical Physics Letters*, *26*(2), 163-166. https://doi.org/https://doi.org/10.1016/0009-2614(74)85388-1

Girel, K. V., Panarin, A. Y., Bandarenka, H. V., Isic, G., Bondarenko, V. P., & Terekhov, S. N. (2018). Plasmonic silvered nanostructures on macroporous

Ref. code: 25655922300099OUH

silicon decorated with graphene oxide for SERS-spectroscopy. *Nanotechnology*, *29*(39), 395708. https://doi.org/10.1088/1361-6528/aad250

Guo, J., Zhong, Z., Li, Y., Liu, Y., Wang, R., & Ju, H. (2019). "Three-in-One" SERS Adhesive Tape for Rapid Sampling, Release, and Detection of Wound Infectious Pathogens. *ACS Applied Materials & Interfaces*, *11*(40), 36399-36408. https://doi.org/10.1021/acsami.9b12823

Guo, Y., Yu, J., Li, C., Li, Z., Pan, J., Liu, A., . . . Zhang, C. (2018). SERS substrate based on the flexible hybrid of polydimethylsiloxane and silver colloid decorated with silver nanoparticles. *Optics Express*, *26*(17), 21784-21796. https://doi.org/10.1364/OE.26.021784

Hwang, J. S., & Yang, M. (2018). Sensitive and Reproducible Gold SERS Sensor Based on Interference Lithography and Electrophoretic Deposition. *Sensors*, *18*(11), 4076.

Jeanmaire, D. L., & Van Duyne, R. P. (1977). Surface raman spectroelectrochemistry: Part I. Heterocyclic, aromatic, and aliphatic amines adsorbed on the anodized silver electrode. *Journal of Electroanalytical Chemistry and Interfacial Electrochemistry*, *84*(1), 1-20. https://doi.org/https://doi.org/10.1016/S0022-0728(77)80224-6

Jeon, T. Y., Park, S.-G., Lee, S. Y., Jeon, H. C., & Yang, S.-M. (2013). Shape Control of Ag Nanostructures for Practical SERS Substrates. *ACS Applied Materials & Interfaces*, *5*(2), 243-248. https://doi.org/10.1021/am302874d

Jiang, J., Zou, S., Ma, L., Wang, S., Liao, J., & Zhang, Z. (2018). Surface-Enhanced Raman Scattering Detection of Pesticide Residues Using Transparent Adhesive Tapes and Coated Silver Nanorods. *ACS Applied Materials & Interfaces*, *10*(10), 9129-9135. https://doi.org/10.1021/acsami.7b18039

Kim, J., Jang, Y., Kim, N.-J., Kim, H., Yi, G.-C., Shin, Y., . . . Yoon, S. (2019). Study of Chemical Enhancement Mechanism in Non-plasmonic Surface Enhanced Raman Spectroscopy (SERS) [Original Research]. *Frontiers in Chemistry*, *7*(582). https://doi.org/10.3389/fchem.2019.00582

Kumar, P., Khosla, R., Soni, M., Deva, D., & Sharma, S. K. (2017). A highly sensitive, flexible SERS sensor for malachite green detection based on Ag decorated microstructured PDMS substrate fabricated from Taro leaf as template. *Sensors and Actuators B: Chemical*, *246*, 477-486. https://doi.org/https://doi.org/10.1016/j.snb.2017.01.202

Lal, S., Grady, N. K., Kundu, J., Levin, C. S., Lassiter, J. B., & Halas, N. J. (2008). Tailoring plasmonic substrates for surface enhanced spectroscopies. *Chemical Society Reviews*, *37*(5), 898-911. https://doi.org/10.1039/B705969H

Lee, C., Robertson, C. S., Nguyen, A. H., Kahraman, M., & Wachsmann-Hogiu, S. (2015). Thickness of a metallic film, in addition to its roughness, plays a significant role in SERS activity. *Scientific Reports*, *5*(1), 11644. https://doi.org/10.1038/srep11644

Lee, J., Shin, S., Kang, S., Lee, S., Seo, J., & Lee, T. (2015). Highly Stable Surface-Enhanced Raman Spectroscopy Substrates Using Few-Layer Graphene on Silver Nanoparticles. *Journal of Nanomaterials*, *2015*, 975043. https://doi.org/10.1155/2015/975043

Ref. code: 25655922300099OUH

Lee, J. K., Lee, J.-s., Ahn, Y., & Kang, G. (2018). Effect of current density on morphology of silver thin film recovered from crystalline silicon solar cell by electrochemical process. *Thin Solid Films*, *663*, 143-147.

Li, D., Li, D.-W., Fossey, J. S., & Long, Y.-T. (2010). Portable Surface-Enhanced Raman Scattering Sensor for Rapid Detection of Aniline and Phenol Derivatives by On-Site Electrostatic Preconcentration. *Analytical Chemistry*, *82*(22), 9299-9305. https://doi.org/10.1021/ac101812x

Li, J., & Fang, Y. (2007). An investigation of the surface enhanced Raman scattering (SERS) from a new substrate of silver-modified silver electrode by magnetron sputtering. *Spectrochimica Acta Part A: Molecular and Biomolecular Spectroscopy*, *66*(4), 994-1000. https://doi.org/https://doi.org/10.1016/j.saa.2006.05.012

Li, X. (2018). Preparation of Graphene Oxide and Its Application as Substrates for SERS. *Journal of Chemistry*, *2018*, 8050524. https://doi.org/10.1155/2018/8050524

Li, Y.-T., Qu, L.-L., Li, D.-W., Song, Q.-X., Fathi, F., & Long, Y.-T. (2013). Rapid and sensitive in-situ detection of polar antibiotics in water using a disposable Ag–graphene sensor based on electrophoretic preconcentration and surface-enhanced Raman spectroscopy. *Biosensors and Bioelectronics*, *43*, 94-100. https://doi.org/https://doi.org/10.1016/j.bios.2012.12.005

Liland, K. H., Kohler, A., & Afseth, N. K. (2016). Model-based pre-processing in Raman spectroscopy of biological samples. *Journal of Raman Spectroscopy*, *47*(6), 643-650. https://doi.org/https://doi.org/10.1002/jrs.4886

Ling, X., Moura, L. G., Pimenta, M. A., & Zhang, J. (2012). Charge-Transfer Mechanism in Graphene-Enhanced Raman Scattering. *The Journal of Physical Chemistry C*, *116*(47), 25112-25118. https://doi.org/10.1021/jp3088447

Liu, L., Hou, S., Zhao, X., Liu, C., Li, Z., Li, C., . . . Man, B. (2020). Role of Graphene in Constructing Multilayer Plasmonic SERS Substrate with Graphene/AgNPs as Chemical Mechanism-Electromagnetic Mechanism Unit. *Nanomaterials (Basel, Switzerland)*, *10*(12), 2371. https://doi.org/10.3390/nano10122371

Liu, X., Shao, Y., Tang, Y., & Yao, K.-F. (2014). Highly Uniform and Reproducible Surface Enhanced Raman Scattering on Air-stable Metallic Glassy Nanowire Array. *Scientific Reports*, *4*(1), 5835. https://doi.org/10.1038/srep05835

Lucht, S., Murphy, T., Schmidt, H., & Kronfeldt, H.-D. (2000). Optimized recipe for sol–gel-based SERS substrates. *Journal of Raman Spectroscopy*, *31*(11), 1017-1022. https://doi.org/https://doi.org/10.1002/1097-4555(200011)31:11<1017::AID-JRS638>3.0.CO;2-V

López, I., Vázquez, A., Hernández-Padrón, G. H., & Gómez, I. (2013). Electrophoretic deposition (EPD) of silver nanoparticles and their application as surface-enhanced Raman scattering (SERS) substrates. *Applied Surface Science*, *280*, 715-719. https://doi.org/https://doi.org/10.1016/j.apsusc.2013.05.048

Ma, L., Huang, Y., Hou, M., Xie, Z., & Zhang, Z. (2015). Ag Nanorods Coated with Ultrathin TiO2 Shells as Stable and Recyclable SERS Substrates. *Scientific Reports*, *5*(1), 15442. https://doi.org/10.1038/srep15442

Ref. code: 25655922300099OUH

Martynova, N. A., Goldt, A. E., Maslakov, K. I., Savilov, S. V., & Grigorieva, A. V. (2018). Electroplating of porous gold films for SERS analysis of heme derivatives. *Journal of Materials Science*, *53*(11), 7953-7962. https://doi.org/10.1007/s10853-018-2089-7

Nakabayashi, Y., Sakai, H., Suzuki, R., & Yamada, S. (2019). Formation of silver particles for SERS spectroscopy by mist chemical vapor deposition method. In (Vol. 58). Japanese Journal of Applied Physics: IOP Science.

Novara, C., Dalla Marta, S., Virga, A., Lamberti, A., Angelini, A., Chiadò, A., . . . Giorgis, F. (2016). SERS-Active Ag Nanoparticles on Porous Silicon and PDMS Substrates: A Comparative Study of Uniformity and Raman Efficiency. *The Journal of Physical Chemistry C*, *120*(30), 16946-16953. https://doi.org/10.1021/acs.jpcc.6b03852

Park, S.-I., Quan, Y.-J., Kim, S.-H., Kim, H., Kim, S., Chun, D.-M., . . . Ahn, S.-H. (2016). A review on fabrication processes for electrochromic devices. *International Journal of Precision Engineering and Manufacturing-Green Technology*, *3*(4), 397-421. https://doi.org/10.1007/s40684-016-0049-8

Perumal, J., Kong, K. V., Dinish, U. S., Bakker, R. M., & Olivo, M. (2014). Design and fabrication of random silver films as substrate for SERS based nano-stress sensing of proteins. *RSC Advances*, *4*(25), 12995-13000. https://doi.org/10.1039/C3RA44867C

Qiu, H., Wang, M., Jiang, S., Zhang, L., Yang, Z., Li, L., . . . Huang, J. (2017). Reliable molecular trace-detection based on flexible SERS substrate of graphene/Ag-nanoflowers/PMMA. *Sensors and Actuators B: Chemical*, *249*, 439-450. https://doi.org/https://doi.org/10.1016/j.snb.2017.04.118

Reina, A., Jia, X., Ho, J., Nezich, D., Son, H., Bulovic, V., . . . Kong, J. (2009). Large Area, Few-Layer Graphene Films on Arbitrary Substrates by Chemical Vapor Deposition. *Nano Letters*, *9*(1), 30-35. https://doi.org/10.1021/nl801827v

Rivera-Rangel, R. D., Navarro-Segura, M. E., Arizmendi-Morquecho, A., & Sánchez-Domínguez, M. (2020). Electrodeposition of plasmonic bimetallic Ag-Cu nanodendrites and their application as surface-enhanced Raman spectroscopy (SERS) substrates. *Nanotechnology*, *31*(46), 465605. https://doi.org/10.1088/1361-6528/abacf5

Sarkar, A., Wang, H., & Daniels-Race, T. (2014). Surface enhanced Raman spectroscopy on silver-nanoparticle-coated carbon-nanotube networks fabricated by electrophoretic deposition. *Electronic Materials Letters*, *10*(2), 325-335. https://doi.org/10.1007/s13391-013-3147-6

Son, M., & Ham, M.-H. (2017). Low-temperature synthesis of graphene by chemical vapor deposition and its applications. *FlatChem*, *5*, 40-49. https://doi.org/https://doi.org/10.1016/j.flatc.2017.07.002

Song, H., Li, X., Yoo, S., Wu, Y., Liu, W., Wang, X., & Liu, H. (2014). Highly Sensitive Surface Enhanced Raman Spectroscopy from Ag Nanoparticles Decorated Graphene Sheet. *Journal of Nanomaterials*, *2014*, 538024. https://doi.org/10.1155/2014/538024

Soto-Nieto, F., Farías, R., & Reyes-López, S. Y. (2020). Sol–Gel and Electrospinning Synthesis of Silica–Hydroxyapatite–Silver Nanofibers for SEIRAS and SERS. *Coatings*, *10*(10), 910.

Ref. code: 25655922300099OUH

Sun, H., Liu, H., & Wu, Y. (2017). A green, reusable SERS film with high sensitivity for in-situ detection of thiram in apple juice. *Applied Surface Science*, *416*, 704-709. https://doi.org/https://doi.org/10.1016/j.apsusc.2017.04.159

Tzeng, Y., Chen, Y., Lai, J., & Huang, B. (2020). Silver Nanoparticles SERS Sensors Using Rapid Thermal CVD Nanoscale Graphene Islands as Templates. *IEEE Transactions on Nanotechnology*, *19*, 25-33. https://doi.org/10.1109/TNANO.2019.2954490

Wang, K., Sun, D.-W., Pu, H., & Wei, Q. (2021). Polymer multilayers enabled stable and flexible Au@Ag nanoparticle array for nondestructive SERS detection of pesticide residues. *Talanta*, *223*, 121782. https://doi.org/https://doi.org/10.1016/j.talanta.2020.121782

Wang, R., Zhang, L., Zou, S., & Zhang, H. (2019). Electrodeposition of Ag nanodendrites SERS substrates for detection of malachite green. *Microchemical Journal*, *150*, 104127. https://doi.org/https://doi.org/10.1016/j.microc.2019.104127

Wang, X.-l., Zong, R.-l., Shi, S.-k., & Zhu, Y. (2014). Ultrasensitive and reproducible surface-enhanced Raman scattering detection via an optimized adsorption process and filter-based substrate. *Analytical Methods*, *6*(12), 4130-4137. https://doi.org/10.1039/C3AY42153H

Yu, J., Ma, Y., Yang, C., Zhang, H., Liu, L., Su, J., & Gao, Y. (2018). SERS-active composite based on rGO and Au/Ag core-shell nanorods for analytical applications. *Sensors and Actuators B: Chemical*, *254*, 182-188. https://doi.org/https://doi.org/10.1016/j.snb.2017.07.034

Zhang, Y., Yang, C., Xue, B., Peng, Z., Cao, Z., Mu, Q., & Xuan, L. (2018). Highly effective and chemically stable surface enhanced Raman scattering substrates with flower-like 3D Ag-Au hetero-nanostructures. *Scientific Reports*, *8*(1), 898. https://doi.org/10.1038/s41598-018-19165-9

Zhao, M., Guo, H., Liu, W., Tang, J., Wang, L., Zhang, B., . . . Zhang, W. (2016). Silica Cladding of Ag Nanoparticles for High Stability and Surface-Enhanced Raman Spectroscopy Performance. *Nanoscale Research Letters*, *11*(1), 403. https://doi.org/10.1186/s11671-016-1604-5

Zhong, L.-B., Yin, J., Zheng, Y.-M., Liu, Q., Cheng, X.-X., & Luo, F.-H. (2014). Self-Assembly of Au Nanoparticles on PMMA Template as Flexible, Transparent, and Highly Active SERS Substrates. *Analytical Chemistry*, *86*(13), 6262-6267. https://doi.org/10.1021/ac404224f

Zhu, C., Zhao, Q., Huo, D., Hu, X., & Wang, X. (2021). Electrodeposition of rough gold nanoarrays for surface-enhanced Raman scattering detection. *Materials Chemistry and Physics*, *263*, 124388. https://doi.org/https://doi.org/10.1016/j.matchemphys.2021.124388

Zou, Q., Mo, S., Pei, X., Wang, Y., Xue, T., Mayilamu, M., & Qin, G. (2018). Fabrication of novel biological substrate based on photolithographic process for surface enhanced Raman spectroscopy. *AIP Advances*, *8*(8), 085302. https://doi.org/10.1063/1.5039600

Ref. code: 25655922300099OUH

APPENDICES

Ref. code: 25655922300099OUH

APPENDIX A
CALCULATION OF ENHANCEMENT FACTOR OF PDMS SERS SUBSTRATE

In order to calculate the enhancement factor, a 4 µl of 10^{-2} M methyl parathion dropped on PDMS was used to get a normal Raman signal, while a SERS signal was obtained from a 4 µl of 10^{-3} M methyl parathion dropped on a PDMS SERS substrate. The area of the methyl parathion drop on PDMS which was measured after it dried is equal to 7.07 mm^2.

The enhancement factor for SERS can be calculated by

$$EF = \frac{I_{SERS}/N_{SERS}}{I_{NRS}/N_{NRS}} \quad \text{(A.1)}$$

Where I_{SERS} is scattering intensities of SERS

I_{NRS} is the normal Raman scattering

N_{SERS} is the number of SERS probe

N_{NRS} normal Raman probe

The 532 nm laser light coupled through an objective lens of 50× was used as an excitation source. The laser spot area can be calculated by

$$A = \pi r^2 \quad \text{(A.2)}$$

Where r is a radius of laser which was estimated by:

$$r = \frac{1}{2}\left(\frac{1.22\lambda}{Numerical\ Aperture}\right) \quad \text{(A.3)}$$

$$r = \frac{1.22\times 532\ nm}{2\times 0.5} = 0.65\ \mu m \quad \text{(A.4)}$$

Thus, the laser spot area on PDMS is $\pi \times (0.65\ \mu m)^2 = 1.32\ \mu m^2$

Ref. code: 25655922300099OUH

In order to find number of probe molecule N_{NRS}:

$$N_{NRS} = c \times 6.02 \times 10^{23} \times V \quad \text{(A.5)}$$

Where c is a concentration and V is a volume of methyl parathion drop on sample. Therefore, the number of probe molecules of a 4 µl of 10^{-2} M methyl parathion drop on PDMS is:

$$N_{NRS} = 10^{-2} \times 6.02 \times 10^{23} \times 4 \times 10^{-6} = 2.4 \times 10^{16} \text{ molecules} \quad \text{(A.6)}$$

Which is the number of probe molecules in the whole drop area of 7.07 mm^2. However, only the probe molecules under the laser spot (1.32 μm^2) will be considered. Thus, the actual N_{NRS} can be calculated by

$$N_{NRS} = \frac{2.4\times10^{16}\times1.32\times10^{-12}}{7.07\times10^{-6}} = 4.4 \times 10^{9}\ molecules \quad \text{(A.7)}$$

To calculate the number of SERS probe N_{SERS}, only the molecules that involve in SERS process will be considered. It was estimated by assuming that only methyl parathion molecule laid on the gap between metal nanoparticle involve the SERS process, thus it can be estimated by dividing the whole laser spot by the size of methyl parathion (237.6Å) [calculated by DFT with B3LYP hybrid functional].

$$N_{SERS} = \frac{area\ of\ laser\ spot}{size\ of\ MP\ molecule} \quad \text{(A.8)}$$

$$N_{SERS} = \frac{1.32\times10^{-12}}{237.6\times10^{-20}} = 5.56 \times 10^{5}\ molecules \quad \text{(A.9)}$$

The intensity obtained from the experiment of SERS and normal Raman signal on PDMS substrates are 1408 and 754, respectively. Substituting all the parameters in equation A.1 gives the following:

$$EF = \frac{I_{SERS}/N_{SERS}}{I_{NRS}/N_{NRS}} = \frac{1408}{754} \times \frac{4.4\times10^{9}}{5.56\times10^{5}} = 1.48 \times 10^{4} \quad \text{(A.10)}$$

Ref. code: 25655922300099OUH

APPENDIX B
CALCULATION OF ENHANCEMENT FACTOR OF PI SERS SUBSTRATE

The enhancement factor of PI SERS substrate was calculated by using, a 4 µl of 10^{-2} M methyl parathion drop on PI for Raman signal and a 4 µl of 10^{-3} M methyl parathion dropped on PI SERS substrate for SERS signal. An area of the methyl parathion dropping on PI substrate is 37.7 mm^2The laser light at 785 nm coupled through an objective lens of 50× was used as an excitation laser. Thus, the laser spot area on PI calculated by equation A.2 and A.3 is

$$A = \pi \times (0.95\ \mu m)^2 = 3\ \mu m^2 \quad \text{(B.1)}$$

The number of probe molecules of a 4 µl of 10^{-2} M methyl parathion drop on PI substrate calculated by equation A.4 is equal to 2.4×10^{16} molecules. Thus, the number of probe molecule under laser spot is

$$N_{NRS} = \frac{2.4\times10^{16}\times3\times10^{-12}}{37.7\times10^{-6}} = 1.9 \times 10^{9}\ molecules \quad \text{(B.2)}$$

And number of SERS probe calculated by equation A.5 is

$$N_{SERS} = \frac{3\times10^{-12}}{237.6\times10^{-20}} = 1.26 \times 10^{6}\ molecules \quad \text{(B.3)}$$

The intensity obtained from the experiment of SERS and normal Raman signal on PI substrate are 2274.5 and 71989.32, respectively. Substitute all the parameter in equation A.1 gives the following equation:

$$EF = \frac{I_{SERS}/N_{SERS}}{I_{NRS}/N_{NRS}} = \frac{71989.32}{2274.5} \times \frac{1.9\times10^{9}}{1.26\times10^{6}} = 4.7 \times 10^{4} \quad \text{(B.4)}$$

Ref. code: 25655922300099OUH

BIOGRAPHY

Name	Thitima Maturos Daniels
Education	2003: Bachelor of Science (Physics)
	Faculty of Science and Technology
	Thammasat University
	2006: Master of Science (Physics)
	Faculty of Science
	Mahidol University

Publications

Maturos, T., Pogfay, T., Rodaree, K., Chaotheing, S., Jomphoak, A., Wisitsoraat, A., . . . Tuantranont, A. (2012). Enhancement of DNA hybridization under acoustic streaming with three-piezoelectric-transducer system. *Lab Chip*, *12*(1), 133-138. https://doi.org/10.1039/c1lc20720b

Pongpaiboonkul, S., Daniels, T. M., Hodak, J. H., Wisitsoraat, A., & Hodak, S. K. (2021). Preferentially oriented Fe-doped CaCu3Ti4O12 films with high dielectric constant and low dielectric loss deposited on LaAlO3 and NdGaO3 substrates. *Applied Surface Science*, *540*, 148373. https://doi.org/https://doi.org/10.1016/j.apsusc.2020.148373

T. Maturos, K. J., & A. Sappat, T. L., A. Wisitsoraat, P. Wanichapichart, A. Tuantranont,. (2009). Separation and Manipulation of Particles Using Traveling Wave Dielectrophoretic Force. *Advanced Materials Research*, *74*, 219-222. https://doi.org/10.4028/www.scientific.net/AMR.74.219

Ugsornrat, K., Maturos, T., Pasakon, P., Karuwan, C., Pogfay, T., Sriprachuabwong, C., . . . Tuantranont, A. (2018). Electrowetting-on-dielectric chip with integrated screen-printed electrochemical sensor for rapid chemical analysis. *Materials Science and Engineering: B*, *238-239*, 36-41. https://doi.org/https://doi.org/10.1016/j.mseb.2018.12.011

Waiwijit, U., Maturos, T., Pakapongpan, S., Phokharatkul, D., Wisitsoraat, A., & Tuantranont, A. (2016). Highly cytocompatible and flexible three-dimensional graphene/polydimethylsiloxane composite for culture and electrochemical detection of L929 fibroblast cells. In *J Biomater Appl* (Vol. 31, pp. 230-240). © The Author(s) 2016. https://doi.org/10.1177/0885328216656477

Wisitsoraat, A., Mensing, J. P., Karuwan, C., Sriprachuabwong, C., Jaruwongrungsee, K., Phokharatkul, D., . . . Tuantranont, A. (2017). Printed organo-functionalized graphene for biosensing applications. *Biosensors and Bioelectronics*, *87*, 7-17. https://doi.org/https://doi.org/10.1016/j.bios.2016.07.116

Ref. code: 25655922300099OUH